Summer 2021

CODAR's Surface Flow at the Mouth of the Chesapeake Bay: Relation to Bay's and Atlantic's Forcing

Shelby Kathryn Henderson
Old Dominion University, shelbyh.sites@gmail.com

CODAR'S SURFACE FLOW AT THE MOUTH OF THE CHESAPEAKE BAY:

RELATION TO BAY'S AND ATLANTIC'S FORCING

by

Shelby Kathryn Henderson
B.S. May 2015, United States Coast Guard Academy

A Thesis Submitted to the Faculty of
Old Dominion University in Partial Fulfillment of the
Requirements for the Degree of

MASTER OF SCIENCE

OCEAN AND EARTH SCIENCE

OLD DOMINION UNIVERSITY
August 2021

Approved by:

Tal Ezer (Director)

Sophie Clayton (Member)

Sönke Dangendorf (Member)

ABSTRACT

CODAR'S SURFACE FLOW AT THE MOUTH OF CHESAPEAKE BAY:
RELATION TO BAY'S AND ATLANTIC'S FORCING

Shelby Kathryn Henderson
Old Dominion University, 2021
Director: Dr. Tal Ezer

Surface currents in the lower Chesapeake Bay (CB) observed with land-based high-frequency radar antennas, or Coastal Ocean Dynamics Application Radar (CODAR), produce hourly 2D maps of current velocities used for search and rescue, pollution tracking, and fishing operations. This study analyzes the correlations between a 9-year record of surface currents measured by CODAR to coastal sea level, local wind forcing, river discharge into CB, and water transport through the Florida Straits, representing the Gulf Stream's control on sea level along the U.S. mid-Atlantic coast. The goal of this study is to find ways to use CODAR data to detect and monitor long-term sea level changes in CB, which may aide numerical modeling of the lower Bay for long-term forecasting and trend analysis.

Linear regression, spectral and wavelet analyses, and Empirical Mode Decomposition (EMD) are applied to the datasets. Linear regression and spectral analysis show high frequencies of CODAR surface currents driven primarily by winds and link to variations in water levels, while low frequencies explained by river discharge and Gulf Stream. Both spectral and wavelet capture the annual cycle, wavelet suggesting anti-correlation between CODAR outflow and water level at this period. Because these methods only capture signals up to about two years, EMD, which separates lower frequency oscillating modes, is also used. EMD trendlines are qualitatively consistent with known dynamics or may be part of larger decadal oscillations longer than this 9-year dataset. Spectral and EMD agree at high frequencies, but also suggests river and Gulf Stream flow may be linked with CODAR currents on longer time scales. EMD achieves realistic long-term trends and correlations for CODAR, but a longer time series is necessary to produce significant results that could use this data to truly monitor long-term sea level changes for the CB in this manner. The study demonstrated the complex nature and interconnections between the different factors and different time scales affecting the currents at the mouth of the CB. This analysis may be the first of its kind in the attempt at combining all these different observations in a single study.

This thesis is dedicated to my family and many friends
for their unwavering support over these last two years of graduate study.

ACKNOWLEDGMENTS

There are many people who have contributed to the successful completion of this thesis. I extend many thanks to my committee members for their patience and guidance on my research and editing of this manuscript. I would also like to recognize the help of Teresa Updyke for assistance in collecting and organizing the CODAR data. My advisor deserves special recognition for his untiring efforts in analyzing the results of and building this study.

NOMENCLATURE

AMOC	Atlantic Meridional Overturning Circulation
AOML	Atlantic Oceanographic and Meteorological Laboratory
ATON	Aids to Navigation
CB	Chesapeake Bay
CBBT	Chesapeake Bay Bridge Tunnel
CODAR	Coastal Ocean Dynamics Application Radar
CPHN	Cape Henry CODAR Station
EMD/HHT	Empirical Mode Decomposition/Hilbert-Huang Transformation
GIA	Glacial Isostatic Adjustment
GS	Gulf Stream
HF	High Frequency
IMF	Intrinsic Mode Function
MAB	Mid-Atlantic Bight
MARACOOS	Mid-Atlantic Regional Association Coastal Ocean Observing System
NOAA	National Oceanic and Atmospheric Administration
PSD	Power Spectral Density
R	Correlation Coefficient
SLR	Sea Level Rise
SSH	Sea Surface Height
SUNS	Sunset Beach Resort CODAR Station
USGS	U.S. Geological Survey
U-V	Horizontal and vertical component of velocity
VIEW	Ocean View Community Beach CODAR Station

TABLE OF CONTENTS

Page

LIST OF TABLES

LIST OF FIGURES

INTRODUCTION

The lower section of the Chesapeake Bay (CB) is of large interest to many studies as communities along the shores have seen an increased frequency of flooding events in recent years (Ezer & Atkinson, 2014). Flooding during high tides and during storm surges (hurricanes, nor'easters, and tropical storms) are increasing due to the combination of global sea level rise, local land subsidence, ice mass loss, steric expansion, and the potential slowdown of the Gulf Stream, to include ocean circulation changes (more on this later); with large environmental, economic, or human health consequences for communities along the Bay (Boon et. al, 2010; Ezer & Corlett, 2012; Eggleston, 2013). The Chesapeake Bay and its tributaries (see map in Fig. 1) form the largest estuary in the United States; a partially mixed estuary, its mean water depth is about 8 m, is about 280 km in length, and mean width is approximately 23 km (Wang, 1979).

Sea level variability and tides are well documented in the southern Chesapeake Bay, with reliable data dating back to the 1930's. Tides in the lower Chesapeake Bay are mostly semidiurnal, with interactions between the three semidiurnal tidal constituents M2, N2, and S2 (Valle-Levinson et. al, 2001). Generally, the tidal and current range is higher on the eastern shore due to the rotation of the earth and shallow bathymetry (Wells et. al, 1929). The tide enters the Bay with characteristic properties of a progressive wave, that is the maximum flood current occurs near high tide, and the maximum ebb current near low tide (Ahnert, 1960). As the tide proceeds up the Bay, the wave becomes gradually modified.

In the southern Chesapeake Bay, relative sea-level rise (SLR) is especially high due to land subsidence associated with Glacial Isostatic Adjustment (GIA) and local groundwater withdrawal, thus sea level rise has been increasing 3.5 to 4.4 mm/year in the southern Chesapeake Bay (Eggleston et. al, 2013; Boon, 2010). This "hot spot" of accelerated sea level rise is corroborated by another recent study that shows how local sea level rise rates have changed over time from 1-3 mm/year in the 1930's to current rates of 4-10 mm/year spanning the last decade (Ezer & Corlett, 2012). For comparison, global sea levels are estimated to be rising at 1.8 mm/year (Eggleston et. al, 2013). Part of the accelerated SLR is potentially attributed to slowdown of the Gulf Stream (Ezer et al., 2013), as discussed later.

Wind forcing in the lower Chesapeake is seasonal and with the most energetic wind events occurring from north-westerly winds during the late fall and winter and drive surface current flow out of the bay (Valle-Levinson et. al, 2001; Boicourt, 1981). In the summer, there is a shift to predominantly southwest winds that can drive surface current flow northward (into the bay) and can even reverse outward flow if the winds are sufficiently strong and persistent (Boicourt, 1981). It is proposed that tidal and wind forcing have nearly equal importance on current velocities in Chesapeake Bay (Xiong & Berger, 2010; Wang 1979), but their variability and periodicity are very different, as well as their influence on

how currents are changed vertically. In the study conducted here, only surface velocities are considered, and the impact on currents from wind and tides, as well as other factors like river outflows are studied.

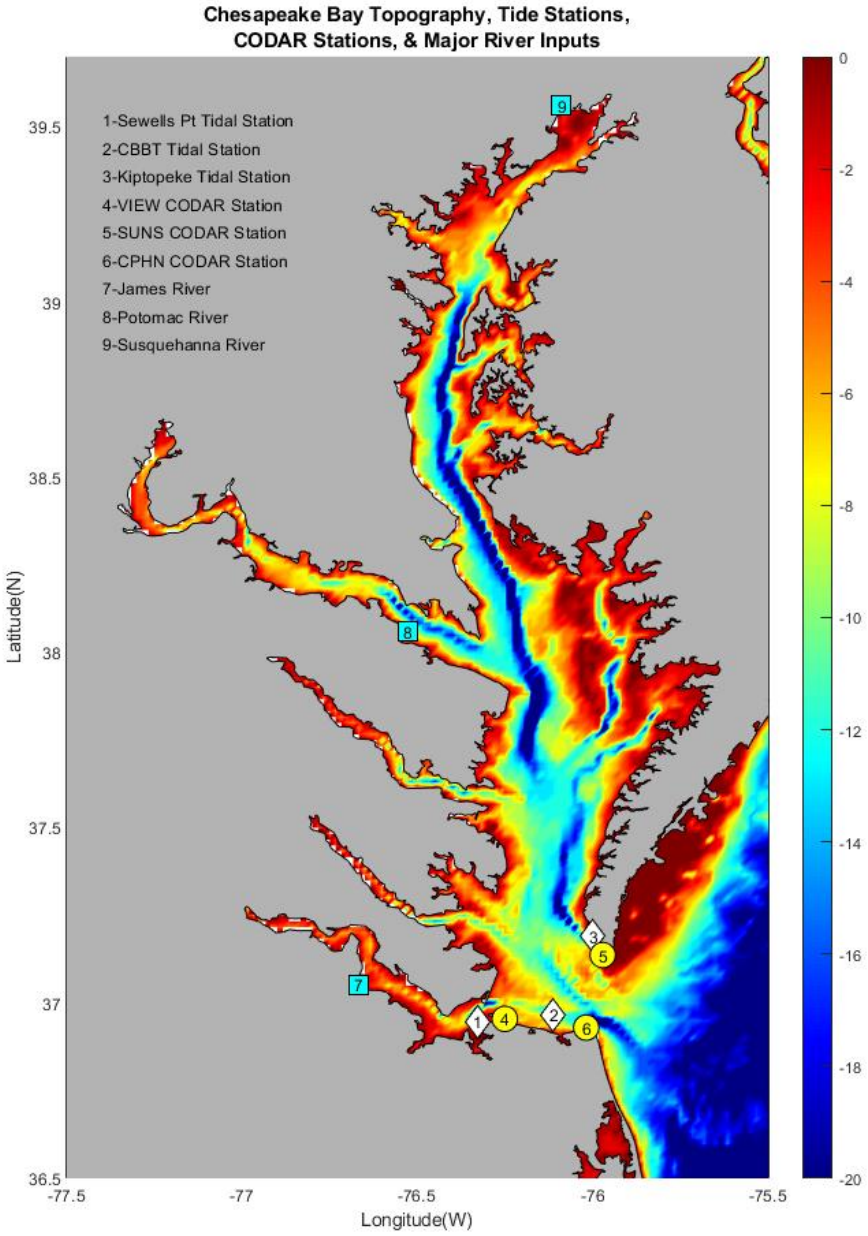

Figure 1: Map of the Chesapeake Bay including topography (obtained from NOAA data), location of tidal stations, HF radars, and river inputs used in the study.

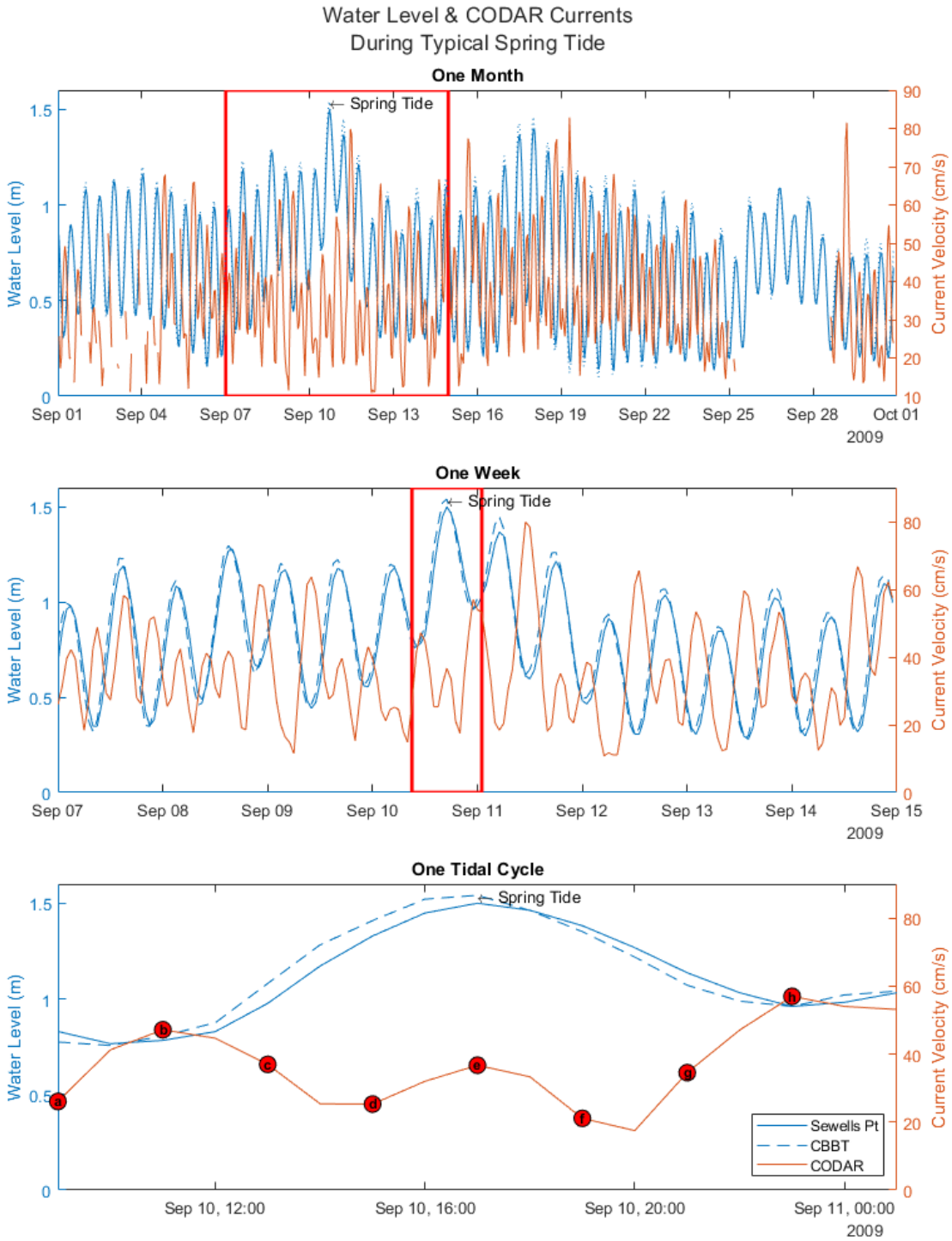

Figure 2: Water level (blue line) obtained from Sewell's Point and CBBBT tidal stations, and CODAR surface current flow out of the bay (red line) are plotted over the course of a typical spring tidal cycle. The second panel shows greater detail about the nonlinear relationship between the two time series. The third panel is a snapshot that is also complements Figure 3, where each marked dot correlates to a 2D velocity map.

More than 80% of the Chesapeake Bay's river input is accounted for by the Susquehanna, Potomac, and James Rivers. The flow of these rivers is consistent with other mid-latitude rivers, with high discharge in the spring, produced by snow melt and spring rains, and low discharge in later summer and early fall (Xiong & Berger, 2010). This in turn creates considerable seasonal variations in salinity throughout the entire of the bay. As for long term trends of river discharge, models and data suggest a climate-related increase in precipitation over the CB watershed, therefore increasing the amount of water transported through the bay (Boomer et. al, 2019). Therefore, the analysis done here of currents at the mouth of the CB may be able to reflect changes in the total river outflows into the CB.

The strength of the Gulf Stream (GS) has been measured since 1982 by the cable across the Florida Strait (Baringer and Larsen, 2001; Meinen et al., 2010). The GS flow is proportional to the elevation gradient across the Gulf Stream at the mid-Atlantic bight (due to the geostrophic balance). When GS flow is weaker, the gradient weakens and thus induces an increase in coastal sea level in the lower Chesapeake Bay (Ezer et. al, 2013). Additionally, the Gulf Stream flow is part of the Atlantic Meridional Overturning circulation (AMOC), which has shown a downward trend of transport since 2004 (Smeed et al., 2014), so a climate related slowdown of AMOC may also affect long-term coastal sea level rise.

This study analyzes various factors such as sea level, wind, river discharge, and speed of the GS to try to understand their links to surface currents in the Chesapeake Bay as measured by the Coastal Ocean Dynamics Applications Radar (CODAR). Also known as SeaSonde, the high frequency (HF) land-based radars are ideal for fine scale monitoring in ports and small bays, with accurate observations up to 70 km (CODAR Ocean Sensors, 2020). The antennas transmit radio signals across the water and receive return signals reflected off waves of a particular wavelength. The measured Doppler shift between the transmitted and received signals allows for calculation of an observed speed. Each antenna site supplies "radials" of current velocity information that is combined with radial information from two or more sites, creating a grid that produces a 2D map of total current velocities (Atkinson et. al 2009). The data are collected for dissemination in near real-time as part of the Mid-Atlantic Regional Association Coastal Ocean Observing System (MARACOOS), and is used to create products available to mariners such as short-term forecasts for shipping channels, pollutant tracking, and as a tool for search and rescue (Atkinson et. al 2009).

Three radars are used in this study that are located in the lower Chesapeake Bay (Fig. 1): one at Norfolk's Ocean View Community Beach (VIEW), the second at the Sunset Beach Resort (SUNS) set on the southwestern tip of the Eastern Shore, and the third at Cape Henry (CPHN). These CODAR stations provide surface currents across the entire mouth of the CB, thus are useful for studying the transports and exchange of water masses between the CB and the Mid-Atlantic Bight (MAB) region of the Atlantic

Ocean. The surface current record spans more than fourteen years from April 2007 to present day, however this study uses data spanning from 01 June 2009 through 31 May 2018. The quality of this data has been verified and proven reliable through comparisons to Doppler current profilers on Aids-to-Navigation (ATON) buoys and observations from a Nortek Acoustic Wave and Current device within the Chesapeake Bay (Atkinson et. al 2009). Between the three radars, current velocities are captured as far north as Cape Charles, VA to the mouth of the Bay, an area roughly 200 square kilometers inside the Bay mouth (Updyke & Atkinson, 2015). An example of a typical CODAR product can be seen in Fig. 3, where the spring tidal cycle is captured and can be seen in the ebb, flow, and rotation of the surface currents.

Analyzing the surface current velocities from CODAR and finding its relationship to sea level, wind, river discharge, and the Gulf Stream transport will help to find ways to use the data to detect and monitor changes in currents and potentially long-term sea level changes in the Chesapeake Bay, as well as other climatic and environmental changes that may affect the health of the CB. Additionally, there is the potential to use the data to aide in numerical modeling of the lower Chesapeake Bay for long-term forecasting and trend analysis. Other implications of changes to surface current include impacts on physical transport and distribution of freshwater throughout the bay, sediments, pollutants, as well as biological exchanges throughout the water column and the estuary-ocean front.

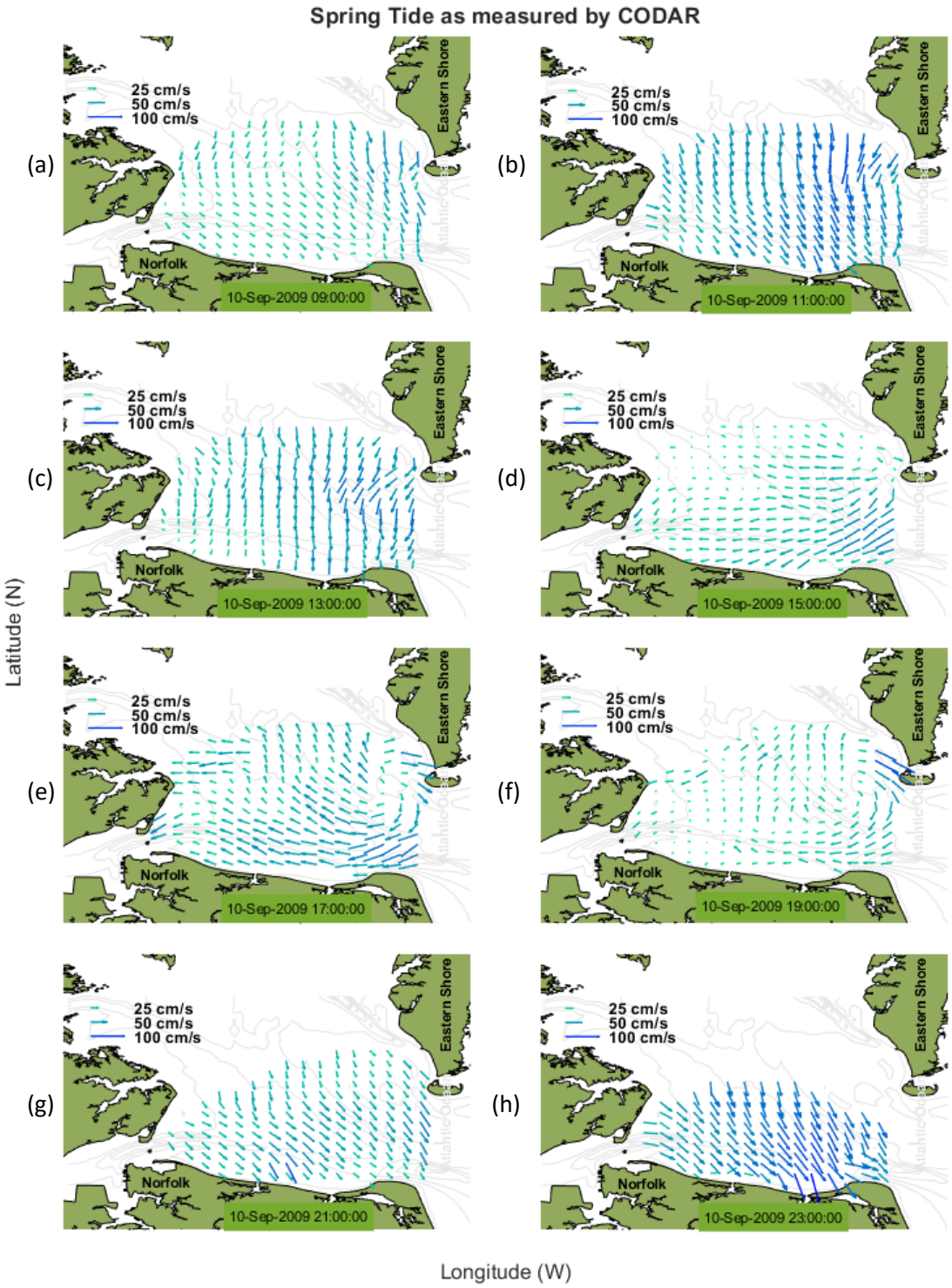

Figure 3: Surface current flow in the lower Chesapeake Bay in illustrative 2-D velocity map. Every two hours is marked on the bottom panel of Fig. 2, and each point corresponds to one of the velocity plots in Fig. 3 through the tidal cycle.

DATA & METHODS

DATA COLLECTION

All data used in this study is publicly available and downloaded through various agency sites or received by request. A summary of the data collected, its source, webpage, and download interval is available in Table 1.

SURFACE CURRENTS

The data collected by the HF-radar is available through Old Dominion University's Center for Coastal Physical Oceanography Surface Current Mapping webpage. The data file format includes latitude, longitude, time, and the U-V components of surface current velocity; data was downloaded in hourly increments from 2009-2018. To analyze the data as a time series, the average is taken over the area (197 points; see Fig. 3) to create a single value for each point in time. It is then transformed so the traditional axis is rotated 45 degrees so that surface currents are analyzed in the Northwest-Southeast directions. By doing so, the horizontal component of surface flow follows the natural geography of the Chesapeake Bay, where negative speeds represent the surface current into the bay, and positive represent current out of the bay. These values are averaged to calculate daily and monthly means that can be compared with daily and monthly data of other observations, without the influence of tidal variability.

WATER LEVELS

Meteorological data and historical water level information were collected from NOAA Tides and Currents webpage. Three water level stations were chosen due to their proximity to the mouth of the Chesapeake Bay and the availability and completeness of the data to include the Chesapeake Bay Bridge Tunnel (CBBT), Sewell's Point, and Kiptopeke stations (Fig. 1). Data were downloaded in 6-minute increments and averaged to calculate daily and monthly water levels. It is important to note, but negligible in terms of data differences, that the CBBT meteorological station was moved in 2017 and the station now stands five miles north of its original location established in 1975. Because the tide station at CBBT is also located on a man-made island used for bridge infrastructure, it has been shown that its sea level trends vary slightly from the Sewell's Point and Kiptopeke coastal stations (Ezer & Corlett, 2012).

WIND SPEED AND DIRECTION

Wind speed and direction data were collected at the CBBT meteorological station and downloaded from NOAA's webpage in 6-minute increments. Data was averaged to calculate daily and monthly wind speeds and directions. The horizontal (U) and meridional (V) components of wind were calculated from the wind speed and direction. The values axis were rotated 45° to the right to match that of the CODAR data, where negative U-values indicate wind into the bay, and positive values indicate wind out of the bay, the same method used to rotate the CODAR data.

RIVER DISCHARGE

Daily river discharge information was collected from three U.S. Geological Survey (USGS) stations to include the Susquehanna River, Potomac River, and James River. These three rivers were chosen because the USGS has established them as the primary freshwater sources to the Chesapeake Bay. The daily data is calculated from current meter measurements in each river. Data from each source is summed and averaged to calculate total monthly mean river streamflow.

FLORIDA CURRENT

Daily water transport from cable measurements at 27°N across the Florida Straits was obtained from NOAA's Atlantic Oceanographic and Meteorological Laboratory (AOML) webpage. The cable measurements are corrected for geomagnetic variations and the tidal signal is removed by NOAA as a standard correction. The data was downloaded in daily increments for the time matching that of the CODAR data from June 2009-May 2018. The dataset was transformed to monthly means to analyze seasonal trends and further data analysis.

Table 1: Summary of data collected for this study, providing source and access links, as well as the download interval used.

Data Type	Source	Access	Temporal Resolution
Surface Currents	Coastal Ocean Dynamics Applications Radar (CODAR)	http://www.ccpo.odu.edu/currentmapping/home.html	Hourly
Water Level	Tidal Stations	https://tidesandcurrents.noaa.gov/	6-minute
Wind Speed & Direction	NOAA's Physical Oceanographic Real-Time System (PORTS)	https://tidesandcurrents.noaa.gov/met.html?id=8638901	6-minute
River Discharge	USGS	https://waterdata.usgs.gov/nwis/uv/?referred_module=sw	Daily
FL Current	NOAA's Atlantic Oceanographic & Meteorological Lab. (AOML)	https://www.aoml.noaa.gov/phod/floridacurrent/data_access.php	Daily

DATA ANALYSIS

The time series of daily and monthly CODAR data is compared to these competing factors in four ways: linear correlation, spectral analysis, Empirical Mode Decomposition (EMD)/Hilbert-Huang Transformation (HHT), and wavelet analysis. Conducting similar analysis using different methods will

provide information on the advantages and limitations of each method, a useful result by itself, besides the physical dynamics of the CB. It should be noted that correlation does not necessarily means cause and effect since several physical processes may be linked to each other in non-linear ways.

LINEAR CORRELATION

The correlation coefficients are computed to measure the direct linear relationship between the CODAR currents and water level, wind, river discharge, and strength of the Gulf Stream spanning the length of the time series of nine years. This analysis neglects lead/lag-relationships between time series and represents the immediate influence one dataset may have on the other. These are compared alongside other methods of analysis' described below.

SPECTRAL ANALYSIS

Standard spectral analysis and coherency is applied to each of the time series. Spectral analysis is a Fourier transform used to partition the variance of a time series as a function of frequency, and contributions from different frequency components are measured in terms of the power spectral density (PSD) (Thomson & Justice, 1998). The PSD estimate is found using Welch's overlapped segment averaging estimator and the frequency with a Hamming window just under 5 days. The upper and lower 95% confidence bounds are calculated using Welch's overlapped segment averaging PSD estimate.

Squared coherence is a measure of the degree of the relationship between two series and is indicated on a scale between 0 and 1, where 0 represents the two time series have no correlation and 1 is an ideal system where the two series are in concert. The cross spectrum is calculated between the CODAR time series and other data, determining the shared power between the two coincident time series (Thomson & Justice, 1998). Phase spectrum indicates the degree to which shared spectral peaks are in phase and is measured in radians or degrees (McDuff and Heath, 2001). Two time series are considered out of phase when the phase difference is ±180º.

EMPIRICAL MODE DECOMPOSITION (EMD)

Spectral analysis only detects oscillations with periods ranging from weeks to a few years within the 9-year record, thus Empirical Mode Decomposition is applied to potentially find oscillations at lower frequency bands (longer periods), including contribution from variability with time scales the length of the record itself. The empirical mode decomposition (EMD)/Hilbert-Huang Transformation (HHT) method is a time series analysis that decomposes the time series data into a finite number of intrinsic mode functions (IMF's) with time-variable amplitudes and frequencies, where the number of modes is determined by the length and variability of the time series (Wu & Huang, 2009). The EMD method was first used to analyze sea level trend in the CB by *Ezer and Corlett* (2012); they used bootstrap simulations to achieve SLR rates accuracy within +/- 0.5 mm/y with 95% confidence level. This study proved that the EMD method is effective in calculating long term trends of datasets even when there is a shorter data

record, whereas standard curve-fitting methods require at least a 60-year record to obtain similar confidence levels of sea level rise (Ezer et. al, 2013).

With this data having a record length of only 9 years, the EMD method is a good approach to detect long term trends within a relatively short dataset. EMD/HHT is calculated for CODAR, water level, wind, river discharge, and Gulf Stream transport data sets from 2009-2018. A significance test is run to find which IMF's are significant within each EMD analysis by comparing the energy spectrum of the decomposed signal (Coughlin, 2005). The EMD of the CODAR is then compared to the EMD of the second time series by calculating a correlation coefficient between the respective IMF's. This indicates which modes (or frequencies) share similar variability.

WAVELET

The wavelet transform is a time series analysis method for dealing with nonstationary oscillations with time-varying amplitudes and phases (Thomson & Justice, 1998). This method decomposes the power of a time series into periodic functions, similar to a Fourier analysis, but using a moving window approach and resulting with wave-like oscillations (Torrence & Compo, 1998). Unlike standard spectral analysis, which generates averaged values of amplitude and phase for each frequency component, the wavelet transform yields a localized, "instantaneous" estimate for the amplitude and phase of each spectral component in the dataset. This gives wavelet analysis an advantage in the analysis of nonstationary data series in which the amplitudes and phases of the harmonic constituents may be changing rapidly in time or space (Thomson & Justice, 1998).

A MATLAB package for multivariate wavelet analysis, developed by Grinsted et al (2004) uses the Morlet wavelet as the mother function, the most used in climate sciences (Grinsted et. al, 2004). Using Monte Carlo simulations, the 95% significance of the power spectrum is determined within each analysis. Cross wavelet transform is calculated to detect phase differences (lag time), non-stationarity, and coherence between CODAR and the other datasets. The coherency calculation shows if the time series share similar power and provides information about correlations at different frequencies.

RESULTS

MONTHLY (SEASONAL), DAILY, AND HOURLY VARIABILITY

It is necessary to analyze the behavior of the different time series on different time scales before calculating correlations or running an analysis, so that seasonal and annual trends can be seen, noted, and further discussed.

DAILY CYCLE

The daily cycle is seen in hourly CODAR currents that show the semidiurnal tidal influence on surface flow within Chesapeake Bay, with a signature double peak indicative of the flood and ebb (Fig. 4). Since the tides are not purely M_2, each day includes 2 high tides with one higher than the other, as seen in Fig. 2. Each peak in Fig. 4 represents the most probable maximum and minimum current speeds (Fig. 4a) and tidal height (representing low and high tide, Fig. 4b) within the bay. For example, winter has the highest mean surface flow (8.5 cm/s), ranging from -25.4 cm/s (into the bay) and 42.4 cm/s (out of the bay); this inflow/outflow is consistent with transport balance of estuaries fed by rivers, so that outflow is larger than the inflow. When these hourly values are averaged to daily values, this tidal variability is decreased (ranges in winter are -1.7 to 18.8 cm/s) and the histograms change their shape closer to that of a normal distribution (Fig. 5). The average daily CODAR velocity through one tidal cycle (half a day) can be seen back in Fig. 2, and the U and V components of velocity are plotted on a 2-D vector map in Fig. 3. Every two hours is marked on the bottom panel of Fig. 2, and each point corresponds to one of the velocity plots in Fig. 3 through the tidal cycle. The relationship between water level and the currents is not strictly linear, and a general pattern appears where there is approximately two peaks in surface current speed for each peak in water height (Fig. 2), because tidal currents peak at both, flood and ebb stages.

The time series from the CBBT, Kiptopeke, and Sewell's Point tidal stations exhibit the expected behavior for a semidiurnal tide and agree with the pattern displayed by CODAR currents, with approximately one high and one low within a 12-hour period (Fig. 2, Fig. 4b). The daily cycle can also be seen in the averaged velocity of the surface currents and the water level time series in the third panel of Fig. 2, where data from both CBBT and Sewell's Point are plotted, indicating a lag of about an hour between the two stations. The relationship between water level and surface currents seen in Fig. 2 is not strictly linear. There are some instances in this time frame that fit the characteristics of the progressive tide that can be best seen in the weekly panel of Fig. 2, where the maximum current and maximum water level occur at the same time. A general pattern can be seen where the average current velocity has two peaks of positive current out of the bay for each peak in water level, but is not without deviations, indicating there are additional non-linear effects effecting the flow.

MONTHLY (SEASONAL) CYCLE

The average annual CODAR flow in the bay is positive due to the net river inflow into the bay, but there are also significant seasonal variations, ranging from 6.1-8.5 cm/s (positive means that flow is moving eastward out of the bay). Seasonally, it is seen that the largest flow occurs in Winter, an average of 8.5 cm/s, versus Summer at 6.1 cm/s (Fig. 4a, Fig. 6a). Also noted is the fact that during summer the distribution of the daily flow is much narrower than during other seasons, indicating smaller variability in the forcing of the flow, as will be seen later when analyzing other data.

The monthly averages of the CODAR time series can be seen in Fig. 6a, along with the monthly averages of the other time series. The largest velocities and variability of CODAR occur in the winter and spring, likely from increased precipitation and snow melt, and the smallest velocities and variability in the summer, as also seen in the histograms of daily data (Fig. 4a-d). This largely agrees with seasonal patterns of wind and river discharge events being greater in the winter and spring, which ultimately influence the strength of the surface flow moving out of the Bay (Xiong & Berger, 2010).

Also plotted in Fig. 6b, is the annual climatology of water level as recorded at Sewell's Point. The monthly average eliminates the daily variability from the constant rise and fall of the tide and presents strong seasonality with water level being highest in the fall and summer, and lowest in the winter and spring. In comparison to CODAR, it looks seemingly inversed; for example, in the summer Chesapeake Bay observes its highest water levels yet the slowest current. The seasonal pattern of sea level was recently analyzed by Ezer (2020) who showed the influence of the annual and semi-annual tidal cycles as well as tropical storms and the weakening of the GS (Fig. 6f)- all these factors can contribute to the peak of monthly sea level in September-October (when the so-called "King Tide" is observed).

Both wind speed and the zonal velocity (U-component) are studied in comparison to CODAR. The U-winds are separated from wind speed and direction because the axis is rotated 45º to the right, thus aligning wind to the surface flow of the CB, having a larger influence than its meridional (V-component) velocity which when rotated, nearly crosses the bay perpendicularly. The histograms (Fig. 5c) have strong seasonal patterns, with greater wind speeds in the winter (mean velocity of 6.4 m/s), and less so in the summer (mean velocity 4.9 m/s). This is largely in part due to energetic storm events with higher wind speeds that are seen more frequently in the winter (Valle-Levinson et. al, 2001). The summer season shows far less speed and variability than the other seasons, as well. The monthly averages of wind speed and zonal velocity were calculated and plotted alongside the other monthly means in Fig. 6c. The same seasonal pattern is observed in the monthly values, with the highest wind speeds and highest variability occurring in the winter.

Streamflow was calculated and averaged from the James, Potomac, and Susquehanna Rivers, which provide more than 80% of freshwater input to the Chesapeake Bay (Xiong & Berger, 2010). The

daily and monthly patterns for river discharge should resemble the patterns seen with the CODAR currents considering the seasonal effect of precipitation and snowmelt increasing flow in the spring. Daily variations of streamflow are highly variable and are seen near as high as 600,000 ft^3/s. Like the other time series, when the monthly average is taken (Fig. 6d), this variability is eliminated. In winter and spring, the average river discharge (e.g. maximum of $9.27x10^4$ ft^3/s in April) has more than four times the average flow in comparison to the summer and fall (e.g. $1.86x10^4$ ft^3/s in August).

Daily values of water transport for the Gulf Stream, as measured by cable across the Florida Strait, indicate strong seasonal flow, with greater water transport and variability in the spring/summer, average of 33 Sv, and the lowest flow occurring in the Fall/Winter, with an average transport of 29.6 Sv. The monthly averages are seen in Fig. 6e, showing this annual cycle. When GS flow is weakened, the SSH gradient across the GS weakens and thus induces an increase in coastal sea level at the MAB region (Ezer et. al, 2013). According Ezer et al. 2013, rise in sea level is related more to the change in slope of the GS rather than to the flow strength itself. Thus, between the maximum GS transport in August and the lowest transport in November (Fig. 6f) there is a persistent weakening of the GS, which could explain the maximum water level in September-October (Fig. 6b).

The river discharge and wind (and more so the u-component) follow the seasonal pattern of CODAR current velocities, i.e., positively correlated and consistent with physical driving mechanisms discussed before (Fig. 6). On the other hand, water level and remote effect of the Gulf Stream could possibly be anticorrelated with CODAR or have a delayed-positive correlation with the surface current velocities.

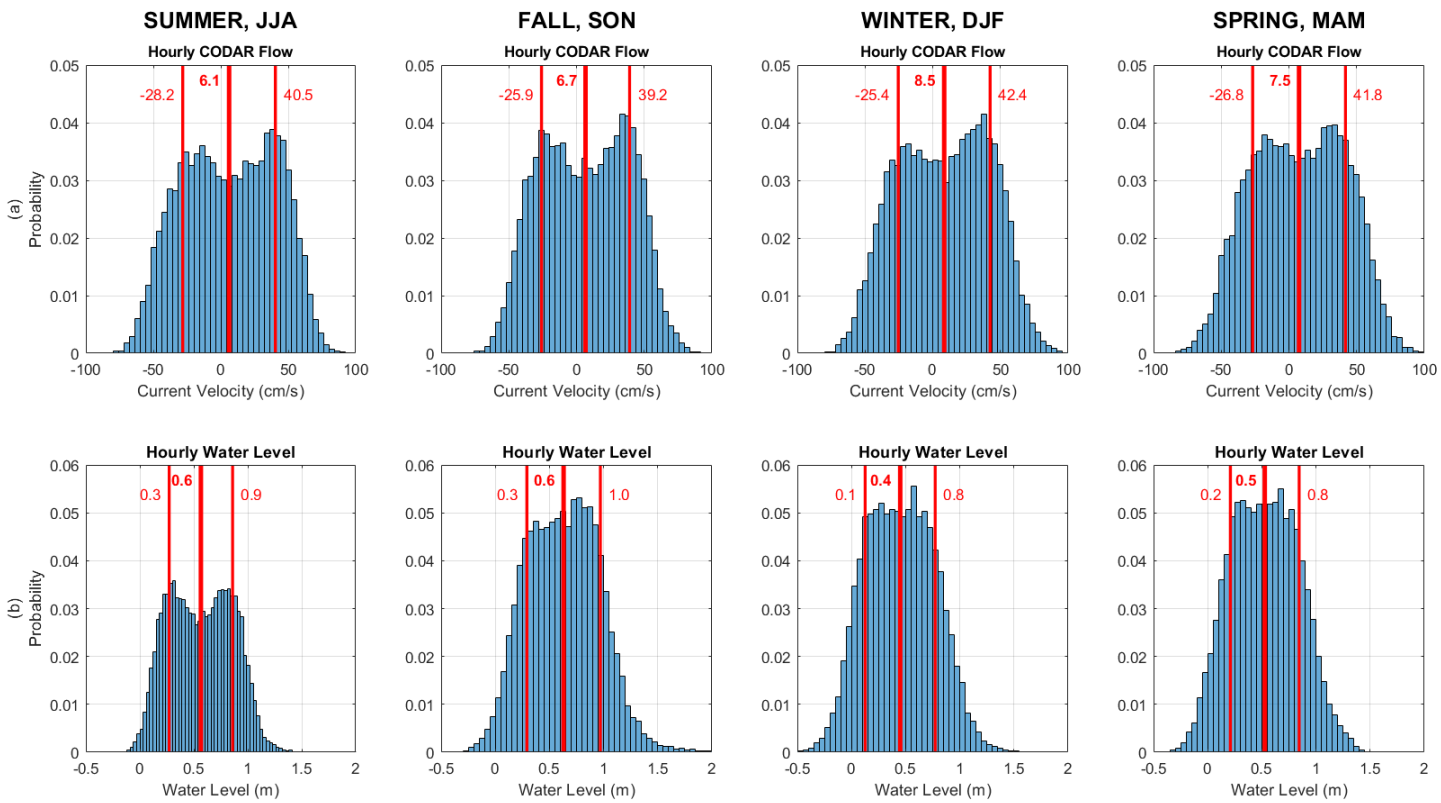

Figure 4: Histograms of hourly CODAR surface current speeds and water levels in Chesapeake Bay. The double peak seen is indicative of the daily high and low tides. Red lines indicate the mean and standard deviations of the datasets.

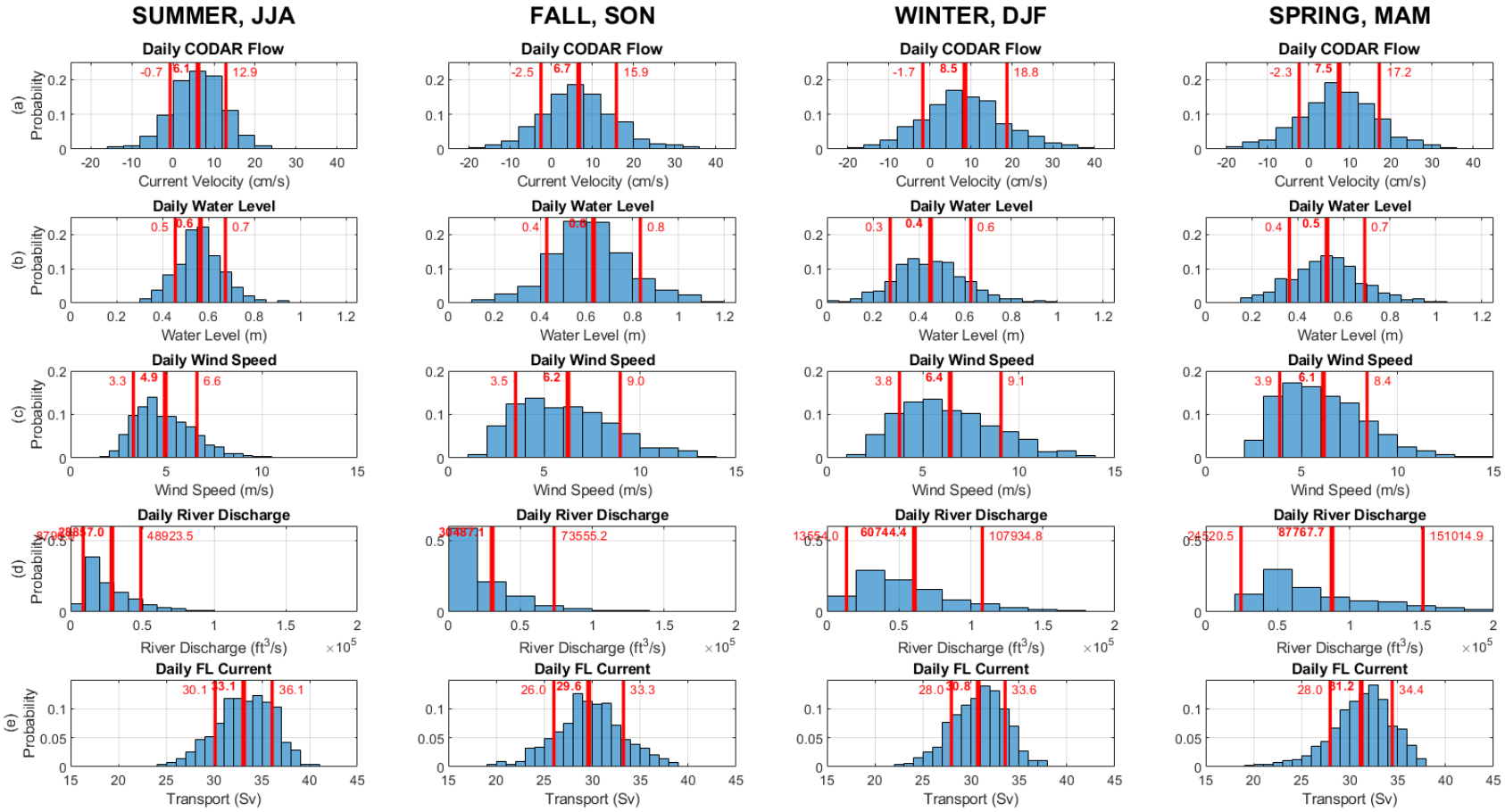

Figure 5: Histograms of the daily CODAR surface current speeds, water level, wind speed, river discharge, and transport of water through the Florida Straits. Tidal variability is eliminated through the average of the current and water level time series. Red lines represent the mean and standard deviations of the datasets.

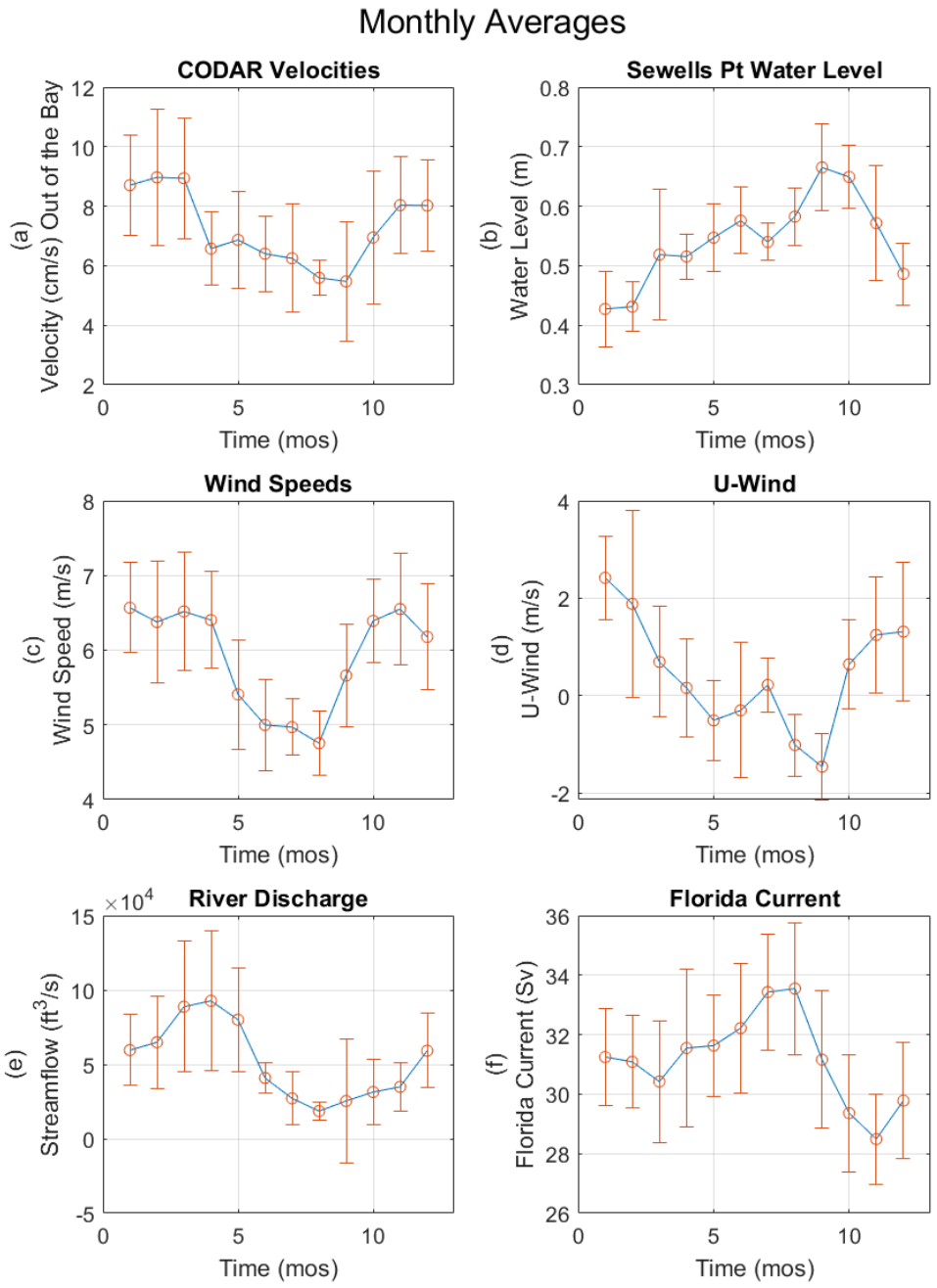

Figure 6: Monthly averages of surface current flow as collected by CODAR, water level at Sewell's Point, wind speed, zonal wind speed, river discharge (from Susquehanna, James, & Potomac), and the transport of the GS (from cable across FL strait). Blue lines represent the monthly average, orange lines represent the standard deviations.

LINEAR CORRELATION

Correlation coefficients were calculated comparing daily CODAR values to each of the factors measured in the Chesapeake Bay and displayed in Table 1, along with the p-value, and upper and lower bounds of the correlation for 95% significance level. This study did not calculate a lag-linear correlation between the time series, which may impact the relationship seen between the variables. The goal here is to assess the factors which influence the surface currents in the Bay directly; assessing links on different time-scales will be done later using other statistical methods.

Based on the time series alone, the highest linear correlation of CODAR is to the daily U-Wind (speed and direction), followed by wind speed, which due to the rotated axis, blows northwest to southeast, the direction of flow in and out of the Chesapeake Bay. In the late fall and winter, when winds are most energetic and primarily from the northwest, the wind pushes water out of the bay and the two are most correlated, versus the summer when winds from the south may work against flow moving out of the Bay (Boicourt, 1981).

There is positive correlation between river discharge and surface flow, which is statistically significant at the 95% level, but R is relatively small, so rivers only contribute small percentage to daily variations in CODAR currents (compared with much larger contribution to the seasonal cycle seen in Fig. 6). Nevertheless, overall addition of freshwater to the estuary does contribute to more flow out of the Bay as expected. An anti-correlation (though with small R) exists between CODAR and the transport of the Florida Current, which is linked more strongly to water level than to currents (Ezer et. al, 2013). The smallest linear correlations are to the water level measured inside the Bay from the three tide gauge stations. While a typical understanding of the relationship between water level inside the Bay and the surface currents is usually anti-correlated (lower water level allows increased flow out of CB), as discussed previously, the tides and maximum current frequently occur at the same time due to the progressive nature of tides in the lower CB and the two can be positively correlated, and the relationship is not certain (Fig. 2). It seems that water level is much better anticorrelated with CODAR currents on hourly-tidal basis (Fig. 2) and on monthly-seasonal basis (Fig. 6a-b) than it does on daily mean basis (Table 1).

SPECTRAL ANALYSIS

Standard spectral analysis is applied to each time series and plotted in Fig. 7 and the squared coherence and cross spectrum phase are plotted in Fig. 8. Note that lags in a phase spectrum are expressed in degrees rather than in days, as the lag is a function of frequency. Positive phase means that the second variable lags the CODAR currents. The phase (lag time) (days) = period of the spectral peak ($2\pi/f$) * Lag (degrees)/360 (McDuff and Heath, 2001).

Table 2: Correlation coefficients (R), p-value (P) and their lower and upper confidence interval for 95% significance (RL and RU), comparing daily CODAR current velocities outflow to different measurements (see text for details).

	Sewell's Point (m)	CBBT (m)	Kiptopeke (m)	U Wind (m/s)	V Wind (m/s)	Wind Speed (m/s)	River Discharge (ft^3/s)	Florida Current (Sv)
R	0.0957	0.1046	0.0633	0.5404	-0.0712	0.2575	0.1144	-0.1124
P	0	0	0.0003	0	0.0001	0	0	0
RL	0.0612	0.0701	0.0287	0.5144	-0.1070	0.2248	0.0800	-0.1468
RU	0.1299	0.1388	0.0978	0.5655	-0.0352	0.2896	0.1486	-0.0776

POWER SPECTRAL DENSITY (PSD)

Simply looking at the power spectral density plots (Fig. 7), each time series indicates strong power on the annual scale, with relatively decreasing power as the frequency increases. Each spectral analysis has a similar pattern in the high frequency bands that share similar slopes and could be estimated via linear regression.

The spectrum for CODAR (Fig. 7a) indicates maximum power at two frequency bands: at the one-year mark in the low frequency spectrum, and a secondary maximum at the one-week mark in the high frequency spectrum. There is also a small peak in power in the CODAR data around the six-month period, and reduced power around the three-month and one-month frequencies. The low energy in the middle of the CODAR spectrum (period of few weeks to few months) is peculiar in that is lower in comparison to the other time series.

A similar pattern is seen in the wind and water level spectrums (Fig. 7b-c-d), with two maximums at the annual scale, and a second maximum at about a month. There is also similar reduction of energy in these spectrums at the three-month frequency, though not as dramatic, indicative of the seasonality of wind speed and coastal sea level.

COHERENCE AND CROSS SPECTRUM PHASE

The surface currents show significant coherence to coastal sea level at higher frequencies in the hourly to weekly frequency bands (Fig. 8a). The cross-spectrum phase only indicates phase with significant coherence based on the degrees of freedom in the hamming window, with $C^2 > 0.55$. Phase is negative between CODAR and sea level, meaning that the water level is driving the surface currents at these high frequencies. The range of the phase is variable, from near in phase (0^o) to near out of phase (-137^o at its greatest) at near weekly time scales. If truly out of phase (180^o), the relationship between water level and the currents would be reversed, that is higher water levels would indicate slower surface

velocities, and vice versa for the series exactly in phase. When in phase, it is likely a direct representation of the positive and negative tidal influence on the surface currents.

CODAR currents are significantly coherent with the wind spectrums on the annual scale (see Fig. 8b-c), as well as high frequency scales less than one month. The cross spectrum phase is largely negative (meaning the winds drive the currents at these frequencies), and the lag at its greatest is less than two weeks, which may require further study.

The river discharge is largely coherent with the surface currents on the annual and three-month time sales, with little correlation at high frequencies. The river streamflow leads the CODAR currents (negative cross spectrum phase) with lag of approximately 17 days at just over the monthly frequency (Fig. 8d). On the annual scale, there is a positive phase, which may be indicative of a shared seasonal pattern.

Similarly, there is a large coherence (but positive cross spectrum phase) between CODAR and the Gulf Stream at the annual frequency. Normally a positive phase would indicate the surface currents are leading the GS, however being so close to out of phase (140^{o}, meaning lag of approximately 132 days) it can easily be the other way around with changes in the GS affecting the surface currents in the lower CB. The two series are also close to out of phase at time scales less than a month.

Overall, the spectral analysis shows that high frequency (short time scale) oscillations of CODAR are driven by local tide and wind forcing, while the low frequency oscillations, greater than 3 months, are more likely explained by the indirect forcing of river discharge and the Gulf Stream. Since our data set is only nine years in length, the spectral analysis only captures signals up to two years, so further analysis is applied to attempt to detect power on longer time scales.

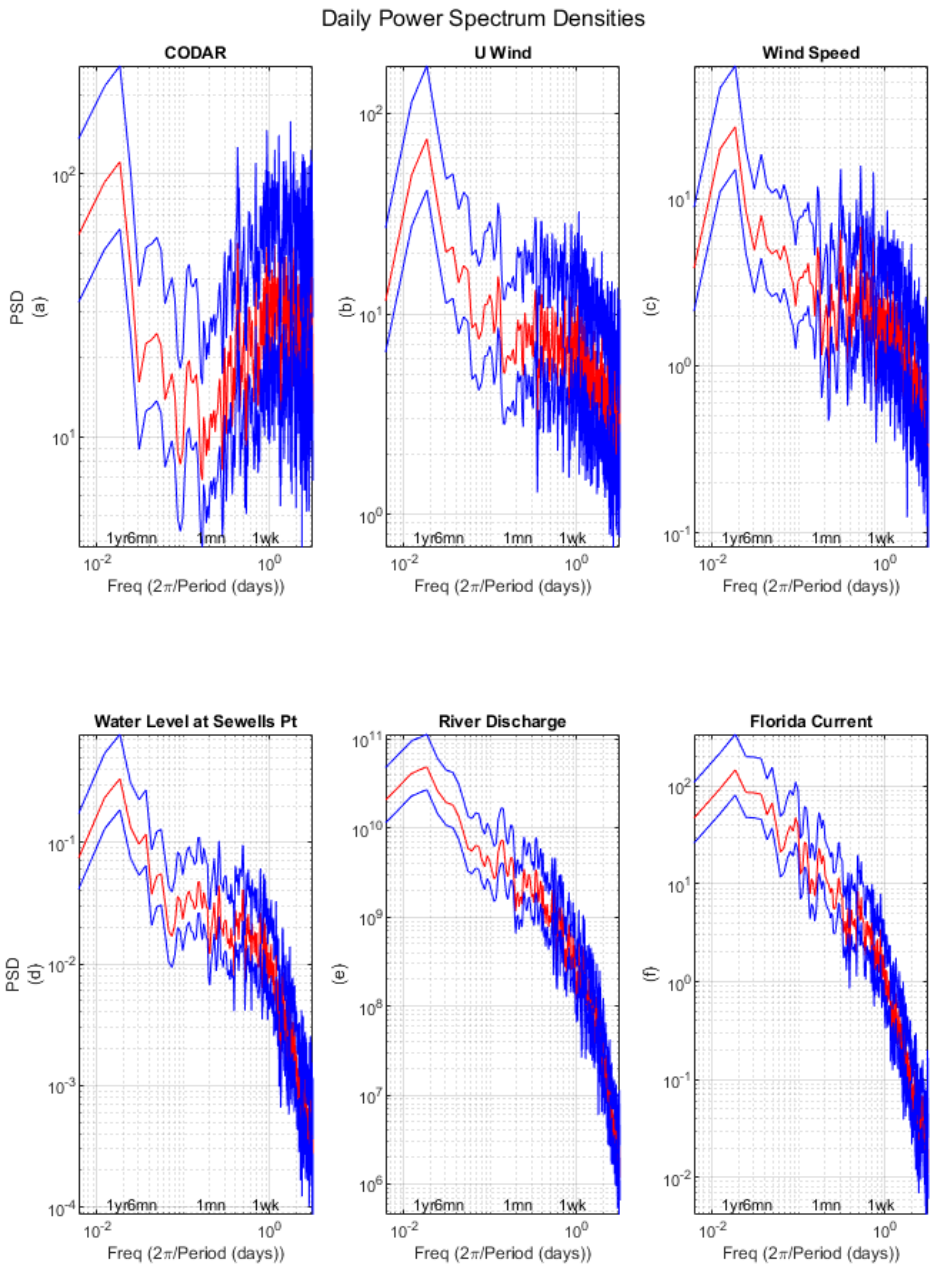

Figure 7: The power spectral density is plotted on the y-axis and frequency on the x-axis. Power spectra indicated by red lines. Blue lines indicate the 95% confidence interval. Periodic oscillations and patterns can be seen within each time series.

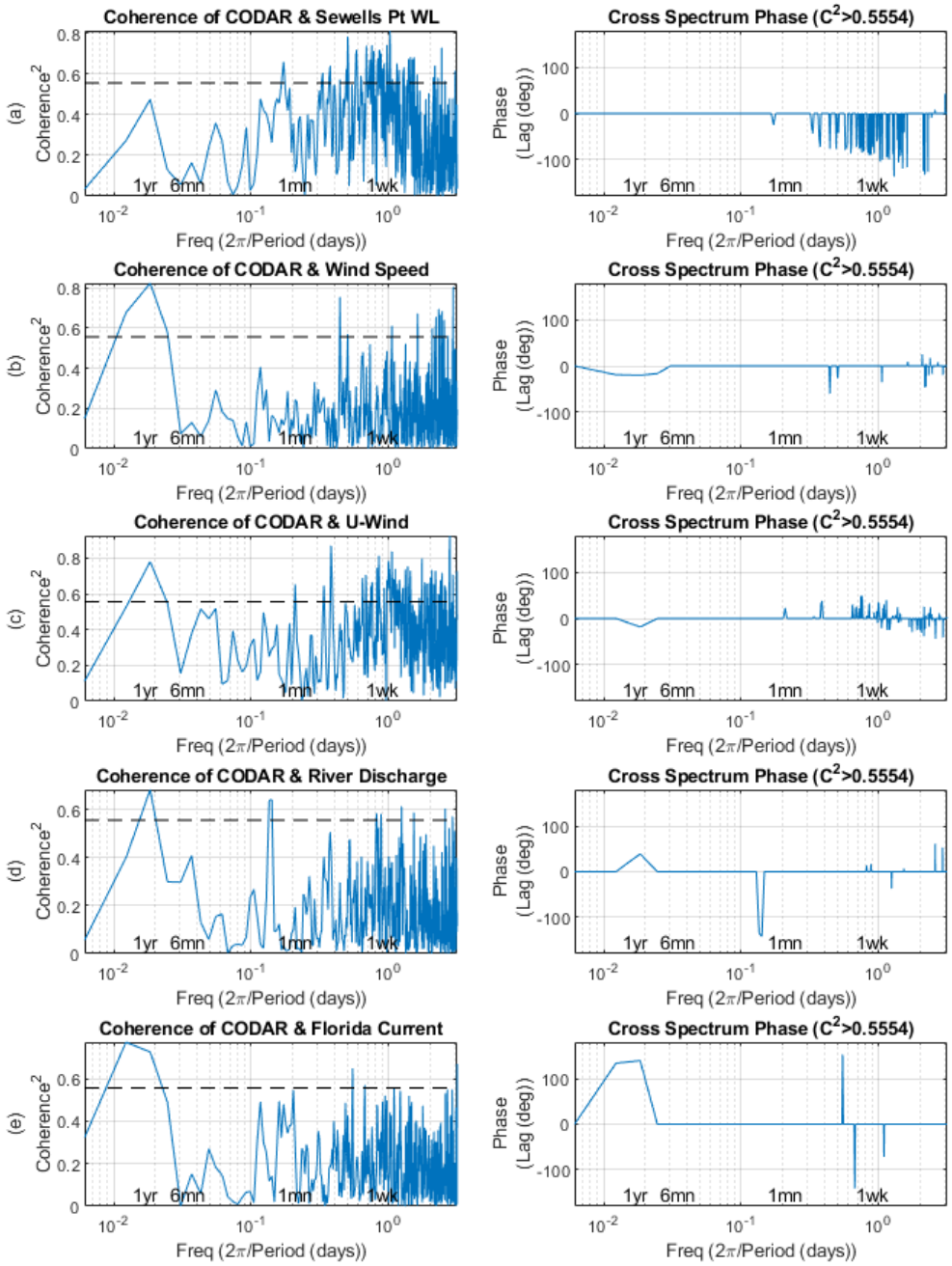

Figure 8: The left-hand column displays the squared coherence between the power spectra of the different time series, a measure of how well they are correlated at different frequencies. Dash line indicates estimated 95% confidence. On the right is the phase difference between the two time-series, indicating which time series leads the other and if there is any lag.

EMPIRICAL MODE DECOMPOSITION (EMD)

Empirical Mode Decomposition (EMD) is an analysis method that separates the long-term trend from oscillating modes long term cycles with periods longer than the record itself where only part of the cycle is captured by the data can contribute to the trend. In Ezer & Corlett (2012), EMD was used to detect non-linear acceleration in sea level trend for the first time within the Chesapeake Bay. This analysis method is applied to the surface currents time series collected by CODAR to detect any long term or interannual trends within the time series, as well as to the previously discussed water levels, winds, river discharge, and Gulf Stream transport. Cross correlations are calculated between the CODAR and other datasets at each mode to detect any correlations on longer time scales between the different time series.

INSTRINSIC MODE FUNCTIONS

The daily time series produced EMD analyses with 11 Intrinsic Mode Functions (IMF's or simply referred to as EMD modes), and the monthly time series produced EMD analyses with 6 IMF's, with the final IMF in each representing the overall trend. An example of two of the daily EMD analyses can be seen in Fig. 9, where the blue line represents the IMF of the CODAR currents, and the red line represents the IMF of the water level at Sewells Point. Mode 0 is the original monthly data set, and the last mode is the trend. The intrinsic mode functions represent oscillatory cycles with decreasing frequency, but within each mode, the frequency can be time dependent and not restricted to any particular frequency as in spectral methods (Ezer et al., 2013). Oscillations calculated with EMD provide trends on scales 2-4x larger than seen in the spectral analysis.

Because the period of analysis is only nine years in length, it is too short to infer statistically significant long-term trends even with the EMD analysis. A statistical test was run on each IMF for each EMD analysis to show which modes are statistically significant based on their power relative to each other, seen in Fig. 10. This statistical evaluation of confidence level for EMD modes is based on white noise simulations method developed by Wu and Huang (2004). The CODAR time series IMF's only have two frequencies with over 95% significance, which occur at the annual time scale and the daily time scale (Fig. 10a). On the other hand, the other time series have more significant modes, meaning the behavior of the EMD analysis are more representative of their seasonal and interannual oscillations. Still, each dataset remains significant on the annual scale, meaning correlations at this frequency specifically may produce more realistic trends or significant correlations when compared to CODAR. It is possible that because of the different forcing sources on the CODAR currents, some of the EMD modes that are not statistically significant are influenced by opposing forcing.

Even if not statistically significant, qualitatively, some of the trend oscillations are consistent with the dynamics involved; none of the trends are linear, pointing to impacts from decadal and longer

oscillations. For example, the final IMF (representing the long-term trend) for each analysis are plotted in Fig. 11. (Trends produced using the monthly IMF's are not plotted, as their shape is the same as produced by the daily IMF's.) The trendlines for water level and river discharge predict an increase, which is expected as previously discussed. Dynamically, it is understood that water level and surface currents are anticorrelated as explained before, so when water level decreases in the estuary, more water flows out of the bay (increasing surface currents), and the final mode (mode 11) shows this within the EMD analysis (Fig. 11) with an average correlation R= -0.43. The trend of the wind data show unclear fluctuations and appear largely constant, with U-wind and total wind speed being interestingly anticorrelated (R= -0.77) to CODAR currents on decadal time scales. Unexpected, and perhaps a result of the shorter time series, is the predicted increase of Gulf Stream transport during this period, with an unusually high correlation (R=0.99, the significance is unclear due to the low degreed of freedom of the smooth trends). The GS is part of the Atlantic Meridional Overturning Circulation (AMOC), which has shown a downward trend of transport since 2004 (Ezer et al., 2013; Smeed et al., 2014). However, the relatively short record analyzed here is likely a reflection of longer unresolved variability like the 8-year cycles of the GS found in previous studies (Ezer et al., 2013). Nevertheless, the trend of increasing CODAR flow out of the bay during this period is consistent with the link to sea level- increase in Gulf Stream transport would cause a local drop in coastal sea level and pull more water out of the Bay, thus suggesting positively CODAR-GS correlated on decadal time scales. The increase in CODAR flow could also be supported by the increase in river discharge, which would also push water out of the Bay. The increase in water level may represent global sea level rise and not necessarily just GS or local forcing. In any case, it is possible that the trends over this short period are just the result of decadal variations of unknown origin and require longer datasets to fully understand and calculate statistically significant trends.

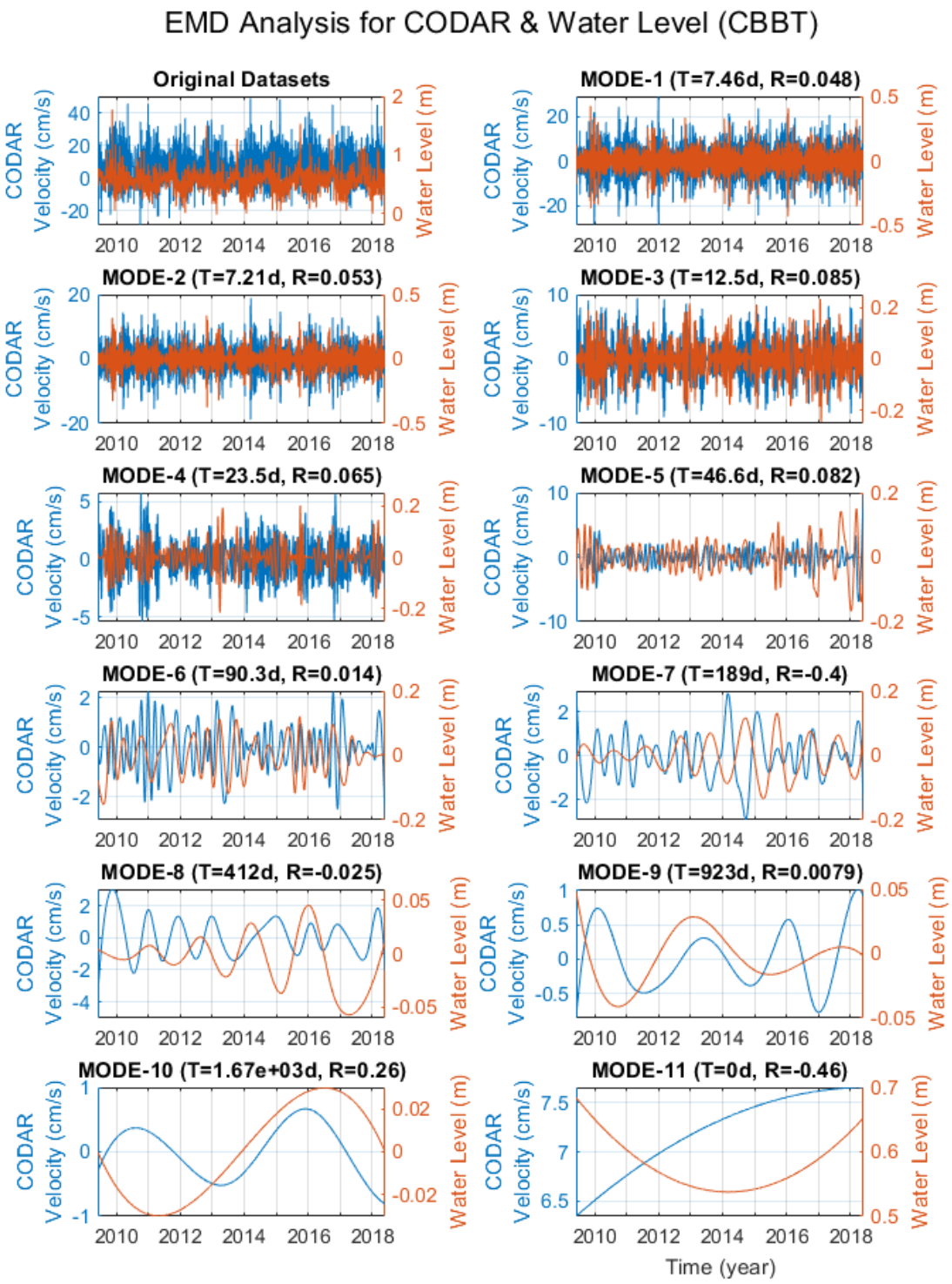

Figure 9: EMD analysis results for surface flow as measured by CODAR (blue) and for water level measured at the CBBT (red). Oscillations are removed and correlation calculated between the two time series at each mode. Mode 0 is the original daily data, and mode 11 is the remaining trend after the 10 oscillating modes have been removed from the original data. Modes with periods less than a year are considered more significant.

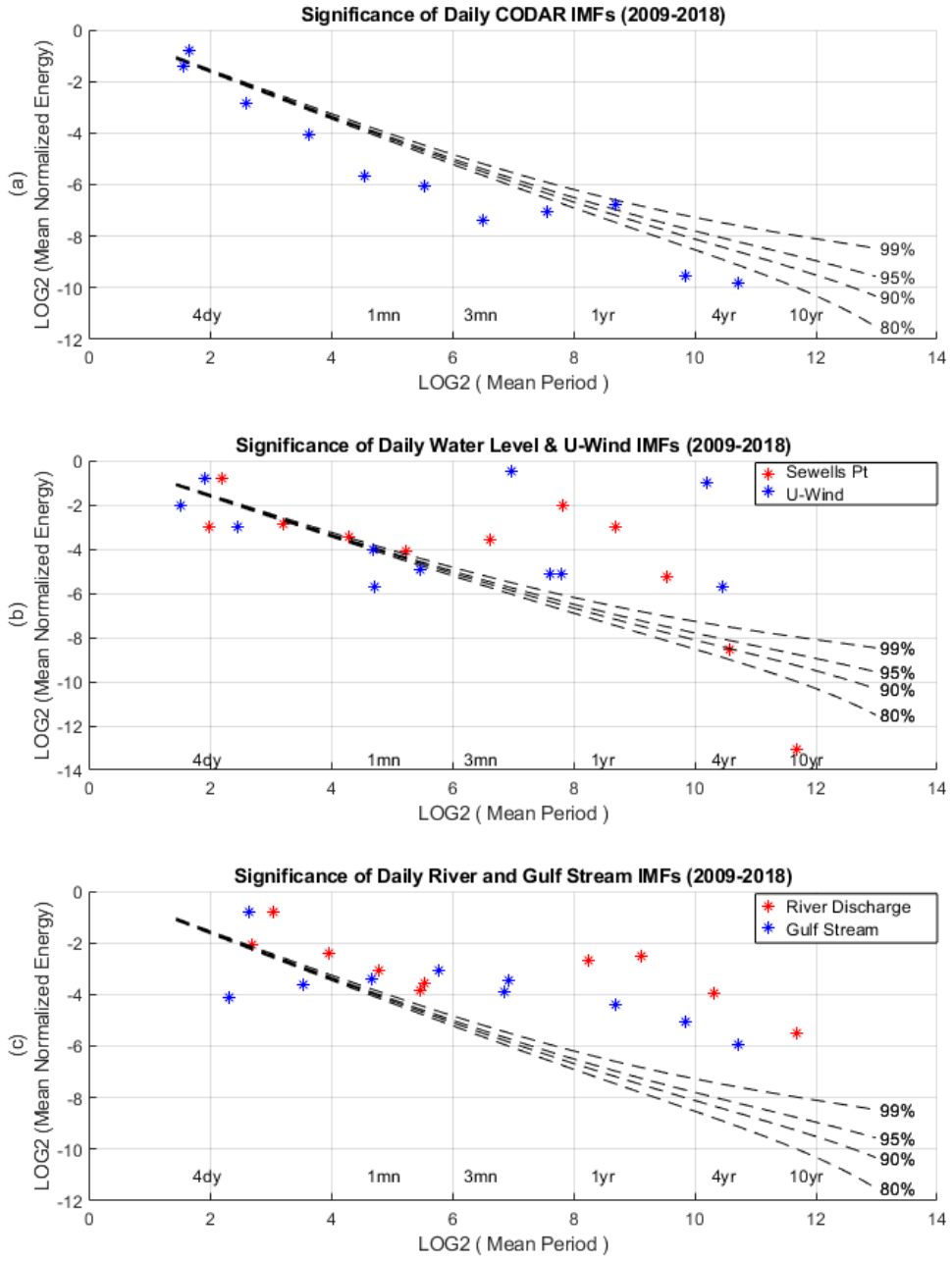

Figure 10: Significance test results for each IMF of the EMD analyses for the daily records of the different time series. CODAR flow out of the bay indicates significance only on the annual and daily scales.

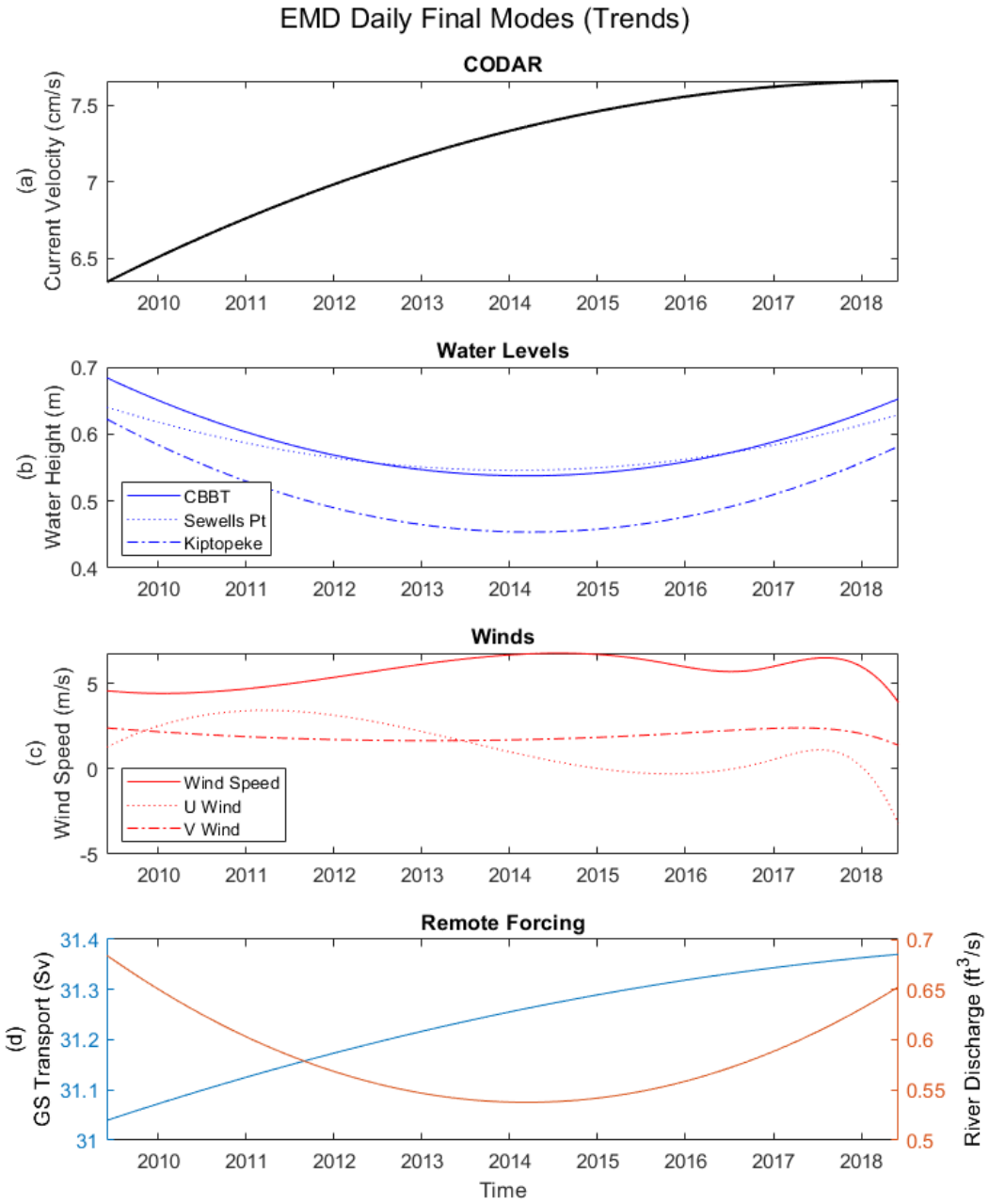

Figure 11: The last IMF of the EMD calculation is plotted for each time series and represents the predictive trend or a part of an unknown decadal oscillation.

CROSS CORRELATIONS

Cross correlations are calculated between each IMF from the CODAR dataset to the corresponding IMF of the second time series (water level, wind, rivers and GS) to see how the links between variables may depend on time-scales. The correlations (R) between CODAR and the other time series for each IMF are plotted together in Fig. 12 (daily) and Fig. 13 (monthly). Note that linear correlation coefficients (Table 2), were not calculated for the monthly data and for the trends due to the lower degrees of freedom in these cases. The daily analysis provides more information about correlations at higher frequencies (or shorter time scales), with a maximum correlation at 1,670 days (4.5 years), whereas the monthly averages show more information on correlations at lower frequencies (even larger time scales of 108 months, ~9 years), though data is lost through averaging and may not be statistically significant, it is of interest qualitatively. Significance of these correlations were calculated using autocorrelation and effective degrees of freedom (df reduced at lower frequencies), following the method suggested by Thiebaux and Zwiers (1984).

The three tide gauge stations show similar daily correlations to CODAR (Fig. 12a) with relatively low correlation up to the three month oscillations, and a negative correlation (max R= -0.39) at the six-month frequency, meaning as water level increases, the surface currents decrease on semiannual periods. This could be reflective of the seasonal cycles for the two time series for example, Fig. 6 (the monthly averages) demonstrates the maximum water level occurs at the same time as the minimum average surface current. Interestingly, the tide gauge stations deviate from their similarity after this frequency, where at the interannual scale (about 2.5 years), the Sewell's Point tide gauge indicates a positive correlation (R= 0.4), whereas the Kiptopeke tide gauge station has a negative correlation (R= -0.24). Though this correlation is considered insignificant, perhaps this has to do with the dynamics of how the surface currents move through the bay, Coriolis, or unidentified interannual variations in the local wind pattern. On the annual scale, both the Sewell's Point and Kiptopeke tide gauge stations have positive correlation (R= 0.16 and 0.12, respectively), while the CBBT tide gauge has near zero (R= -0.02) correlation at this frequency. Looking at the monthly correlations (Fig. 13a), high frequencies are not captured in much detail, though show both positive correlations at the highest frequency, and negative correlation around 8 months, similar to the semiannual pattern seen with the daily correlations. The correlations on the annual scale (significant CODAR IMF) also agree with the correlations calculated from the daily data, that is near or above zero. At the interannual period (about 3.5 years), the correlation is negative and becomes even more so in the near decadal period (about 8 years) for all three tide gauge stations (maximum R= -0.78), suggesting that on decadal time scales the two are anticorrelated.

Both the wind speed and the U-component IMF's are compared to the CODAR IMF's; the daily correlations (Fig. 12b) for both are positive at high frequencies modes less than three weeks.

Qualitatively, as wind speed increases out of the Bay (positive U-direction), then the surface currents would also increase out of the Bay as well, so these correlations make sense as their axes are aligned in the same manner. In fact, the U-wind correlations are positive at all modes in the daily analysis until the 4.5-year period, where it becomes unexpectedly anti-correlated (R= -0.31), but at this long time scale this correlation is not statistically significant. The daily overall wind speed (includes both U and V-components) is either positive or, when negative, close to zero over all time scales in these correlations. The monthly IMF correlations (Fig. 13b) for U-wind is positive on time scales less than a year, and near zero starting at a year all the way to the near decadal scale (about 8 years). The monthly wind speed correlations are unusually different in comparison to the monthly U-wind, which may be due to the oscillations of the V-wind component, averaging, or the length of the time series. The wind speed is anti-correlated then to CODAR currents at both the interannual (3.5 years) and near decadal (8 years) time scales, with the maximum negative correlation being R= -0.54 and the 3.5-year period, similar to the anticorrelated trend. At the annual time scale for the monthly correlations, where U-wind is near zero, the overall wind speed correlation to CODAR is largely positive with R= 0.72. The daily correlations are also positive at the annual frequency, however by not such a large amount (R= 0.17), and a thought is the monthly correlations lose data and variability, and therefore accuracy, through averaging.

Comparing the daily river discharge to the CODAR surface currents (Fig. 12c), there is near-zero, though positive correlation between the two until there is a higher correlation (R=0.14) at periods about 45 days, suggesting a lag between river discharge and maximum currents at this time scale. For frequencies increasing after 45 days, the correlation between the two becomes negative, and at the six-months to one-year frequencies (R= -0.19 at both frequencies). A look at the monthly correlations for the two datasets (Fig. 13c), the cross correlation does not capture the high frequency positive correlation at ~1.5 month period, but does depict the semi-annual and annual negative correlations (R= -0.26 at 1.2 years) similar to the daily correlations. Expectedly, on the longer time scales not calculated with the daily IMF's, a positive correlation is seen between the river discharge and surface currents at the lower frequencies corresponding to 3.5 and 8 years, this agree with the concept that currents out of the lower CB do not immediately respond to change in river flow in the upper CB.

The last dataset compared the surface CODAR currents to the strength of the Gulf Stream, a measure of transport through the Florida Straits (Fig. 12c). The daily IMF's show near zero correlation between the two datasets, until the period of ~45 days (R= 0.11), suggesting that at this frequency as GS transport decreases (and the water level would in theory increase, Ezer et. al, 2013), the surface currents in the Bay would also decrease (more flow into the bay). What is interesting though, is that at the ~45-day period, some of the water level stations are positively correlated to the currents as well, which does not necessarily fit the predicted behavior between the three forces. At the semi-annual period, the water level

in the CB is anti-correlated with the CODAR currents (R= -0.36, Fig. 21.c.), which is expected since increase outflow from the CB (positive CODAR) reduces WL in the CB. However, the GS is also negatively correlated (R= -0.39) at this frequency and the negative correlation of CODAR with the Gulf Stream at this time scale is not easily explained. When the GS slows down, the SSH gradient across the GS decreases and coastal sea level increases (Ezer et. al, 2013), but increased WL is associated with negative CODAR outflow (more inflow), thus one expects a positive GS-CODAR correlation. It is possible that at this semiannual time scale other processes are in effect like the seasonal variations of coastal currents or delay response of the CB to changes in the GS upstream. At the annual frequency, the GS shows near zero correlation and negative correlation on the interannual frequency (~2.5 years). The monthly IMF's (Fig. 13c) do not show as much information as the daily at high frequencies but does indicate negative correlation less than 8 months (R= -0.29), agreeing with the daily anti-correlation at the six-month frequency. The low frequencies correlations between CODAR and the GS are near-zero until the near-decadal period (8 years) where it becomes negative (R= -0.86), suggesting that the two are anti-correlated on longer time scales, opposite to what the final trend analysis (Fig. 11) suggests. This may be in part due to the fact that the final IMF is not truly a long-term trend, but rather a shorter period of unresolved longer decadal oscillations.

Overall, the EMD analyses give a lot of complex and not always easily explained information regarding both the individual time series trends over different time scales, as well as their correlations to each other at these different frequencies. A significance test found that the CODAR dataset produced IMF's with more than 95% significance at the high frequency (daily) and annual scales, whereas most of the other datasets had many more significant IMF's at both high and low frequencies (Fig. 10). While not statistically significant, qualitatively, some of the changes seen in the final IMF, representing the trend, are consistent with the dynamics involved to include increasing sea level and river discharge (Fig. 11). Each of these final trends, especially for GS transport (an unexpected increase) and CODAR surface current velocity, may be a part of larger decadal oscillations of unknown origin not captured within this nine-year dataset more so than an overall trend.

The relationship between the high frequency oscillations of CODAR and the other datasets are best seen in the cross correlations of the daily IMF's in Fig. 12, and the low frequency oscillations in the cross correlations of the monthly IMF's in Fig. 13. The high frequency spectrum has predominantly positive correlations to U-wind/wind speed and water level, suggesting that these factors are largely driving the surface currents on time scales of days to weeks. On approximately monthly time scales, river outflow, GS speed, and some of the tide gauge stations have positive correlations, suggesting a positive lag or shared seasonality. At the semi-annual period, the speed of the Gulf Stream and water level are both anti-correlated to the CODAR currents, suggesting that the relationship between the GS and water

level is affected by other processes such as seasonal variations or, as expected, a delayed response between water level and the GS upstream. This does not suggest that at periods of six months, both a decrease in water level and the GS could increase the average surface current velocity out of the bay at the same time, but the processes are occurring at different times with a similar pattern. The annual period has influence primarily from river discharge, wind speed, and some water level. A look at the monthly correlations (Fig. 13) suggest that the low frequency (decadal) oscillations are controlled by local water level, river discharge, and the Gulf Stream. A summation of the information regarding the correlations and their different time scales can be seen in the schematic diagram in Fig. 14; this diagram demonstrates the complex nature of the interconnecting forcing, where at each different time scale different combination of forcing may be in action.

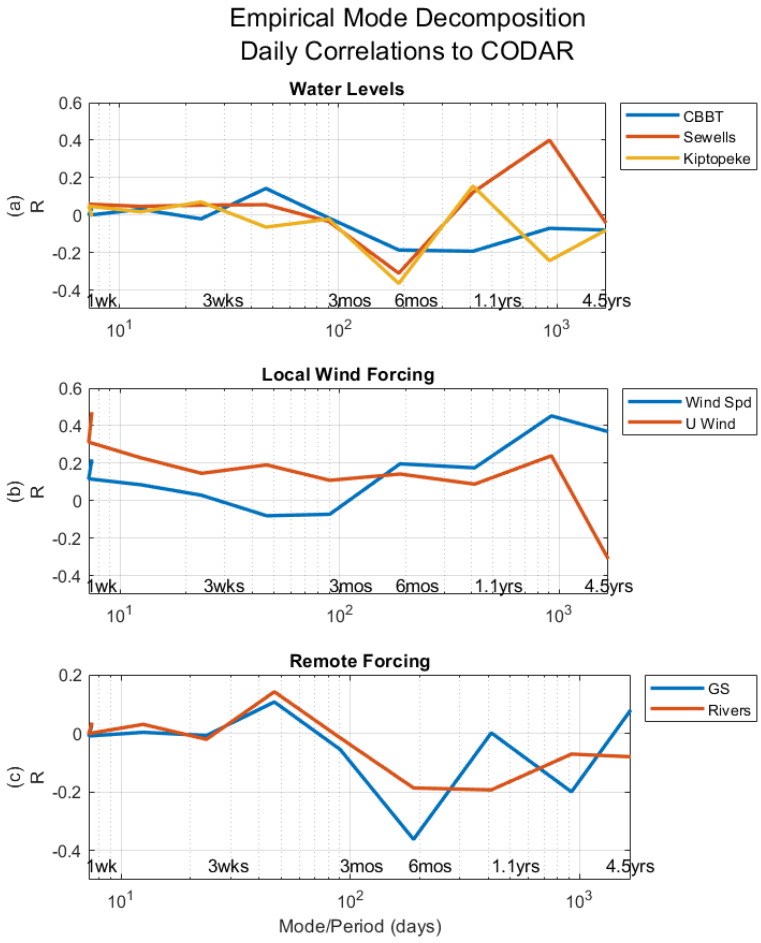

Figure 12: EMD correlations between different time series and CODAR flow out of the bay from 9 year record of daily data. Each mode/period represents a single IMF from the EMD calculation.

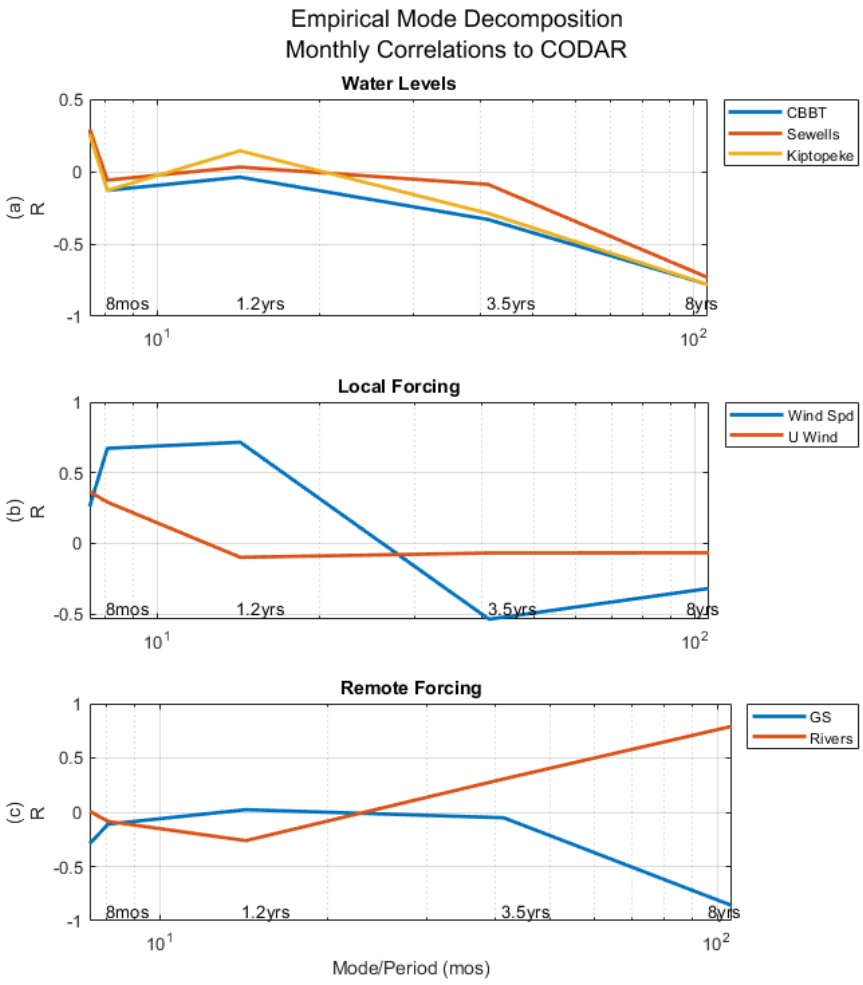

Figure 13: EMD correlations between different time series and CODAR flow out of the bay from 9 year record of monthly data. Each mode/period represents a single IMF from the EMD calculation.

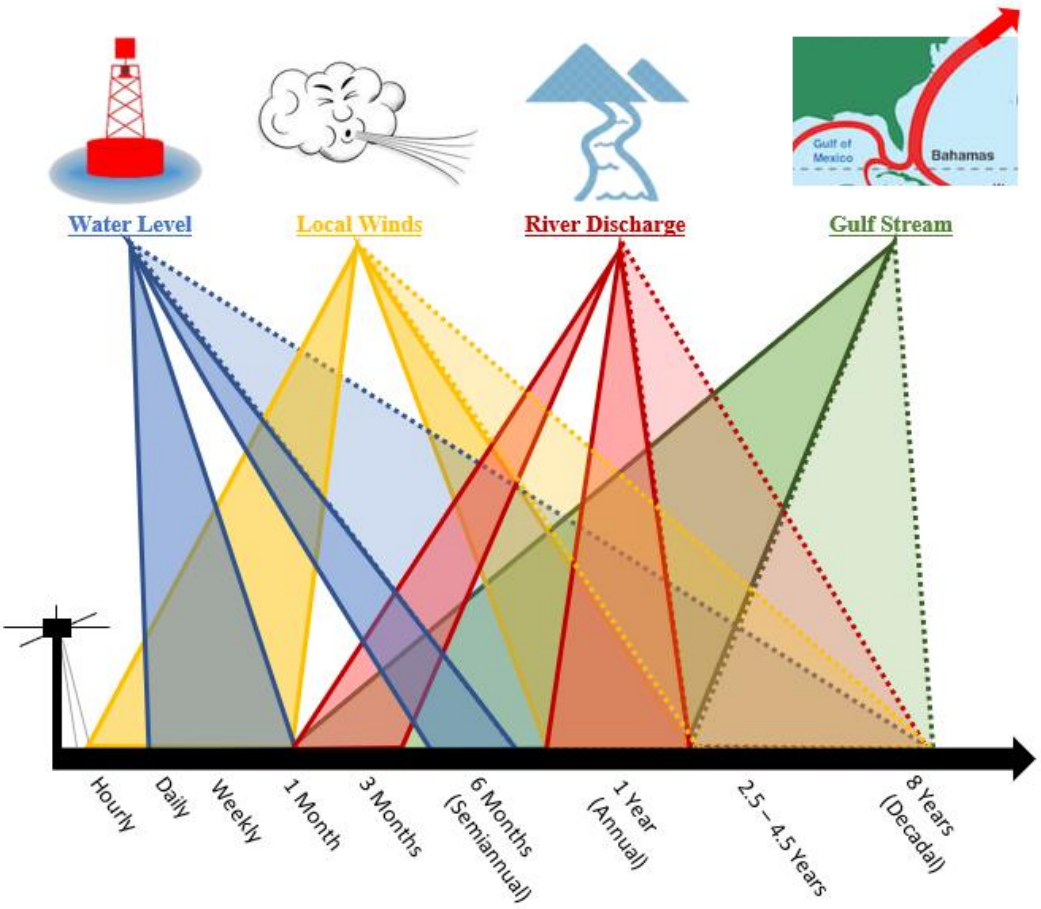

Figure 14: Schematic diagram of EMD correlations to CODAR surface flow out of the Chesapeake Bay on different time scales as calculated by EMD. Solid lined areas represent statistically significant correlations to CODAR found using spectral or EMD analysis. Dotted lined areas represent insignificant or unresolved correlations to CODAR.

WAVELET ANALYSIS

The wavelet transform is a time series analysis method for dealing with nonstationary oscillations with time-varying amplitudes and phases, providing more information about the spectral power over the entire dataset (Thomson & Justice, 1998). This method was only applied to two of the time series, CODAR and water level at CBBT (Fig. 15) to corroborate the findings and correlations calculated using standard spectral analysis and the Empirical Mode Decomposition (EMD) analysis. In the wavelet from the daily CODAR dataset (Fig. 15a), strong power is indicated in yellow, and power with 95% significance is outlined in thick contour, referenced in the wavelet key (Fig. 15d). This indicates that there is a strong annual cycle within the CODAR dataset, and there is significant variability detected at high frequencies, like the significant IMF's detected within the EMD analysis (Fig. 10a). It also appears that there could be some non-stationary patterns occurring on the semi-annual scale within the CODAR time

series as well, as indicated by power around the period of 180 days. The wavelet analysis of the water level time series (Fig. 15b) shows similar power to the CODAR on the annual and high frequencies, but perhaps a more defined semiannual pattern at the 180-day frequency. This is somewhat similar to the spectral analysis (Fig. 7a-d), where CODAR and the water level both have power spectral density (PSD) peaks at the annual period and a smaller peak at the six-month period, as well as a secondary maximum at the one-week period, which is indicated by the thick contours of the high frequency data in Fig. 15.

Cross wavelet transform calculated between the two time series shows that the two time series do share strong power on the annual cycle, and a non-stationary semi-annual cycle as well, both yellow and outlined in thick contour (Fig. 15c). Inside the contour, arrows are pointing directly to the left, meaning the two series are negatively correlated on annual frequencies. In comparison to the daily EMD correlations, this is not necessarily in agreeance with two of the tide gauges which show positive (though small and insignificant) correlation on the annual scale. The spectral analysis did not capture any significant coherence between CODAR and water level on the annual scale, though the correlations have negative phase at higher frequencies. This wavelet suggests coherence not only on the annual scale though, but also variably on the weekly, monthly, and semi-annual frequencies. At periods of 8-60 days, there are non-stationary cycles of coherency (yellow outlined) where the arrows are pointing north/northwest, meaning the tides are influencing the currents, and at a maximum have a lag of 90º, or that is ¼ of the period. For example, at 16 days, the approximate lag between the water level and currents would be four days for this correlation and phase. The wavelet coherency suggests variable influences on the semi-annual scale (180 days), where the arrows alternate up and down through time. Interestingly, the coherency calculation captures a potential non-stationary interannual cycle (about two years), where the two datasets are positively correlated. This is similar to the daily correlations of the EMD analysis compared to Sewell's Point, but opposite to what is seen at Kiptopeke, as well as the monthly correlations which all show a negative correlation at the three-year frequency. The two time series are variable at high frequencies, so it is difficult to distinguish at short time scales how the series are related, whereas spectral analysis and coherence may provide better information at these frequencies.

Overall, the wavelet analysis provides very similar information as to what was seen in the spectral analysis with a peak in power on the annual cycle, a smaller semi-annual cycle, and variable high frequencies. In comparison to the EMD correlations, the wavelet coherency does not necessarily agree at all frequencies. For example, EMD suggests that on the annual cycle the water level and CODAR currents are positively correlated (though not significantly), where wavelet suggests significant anti-correlation. At the six-month period, EMD suggests a negative correlation between the two series, however the wavelet coherence suggests a non-stationary relationship. The daily correlations from EMD also suggest conflicting information about the water level correlation on 2-3 year time scales, whereas the wavelet

coherence shows a significant, non-stationary positive correlation. A thought is that the EMD is unable to resolve the time-varying frequencies as well as the wavelet. Table 3 is constructed to help consolidate and compare this analysis to the spectral and EMD results between the CODAR surface currents and water level.

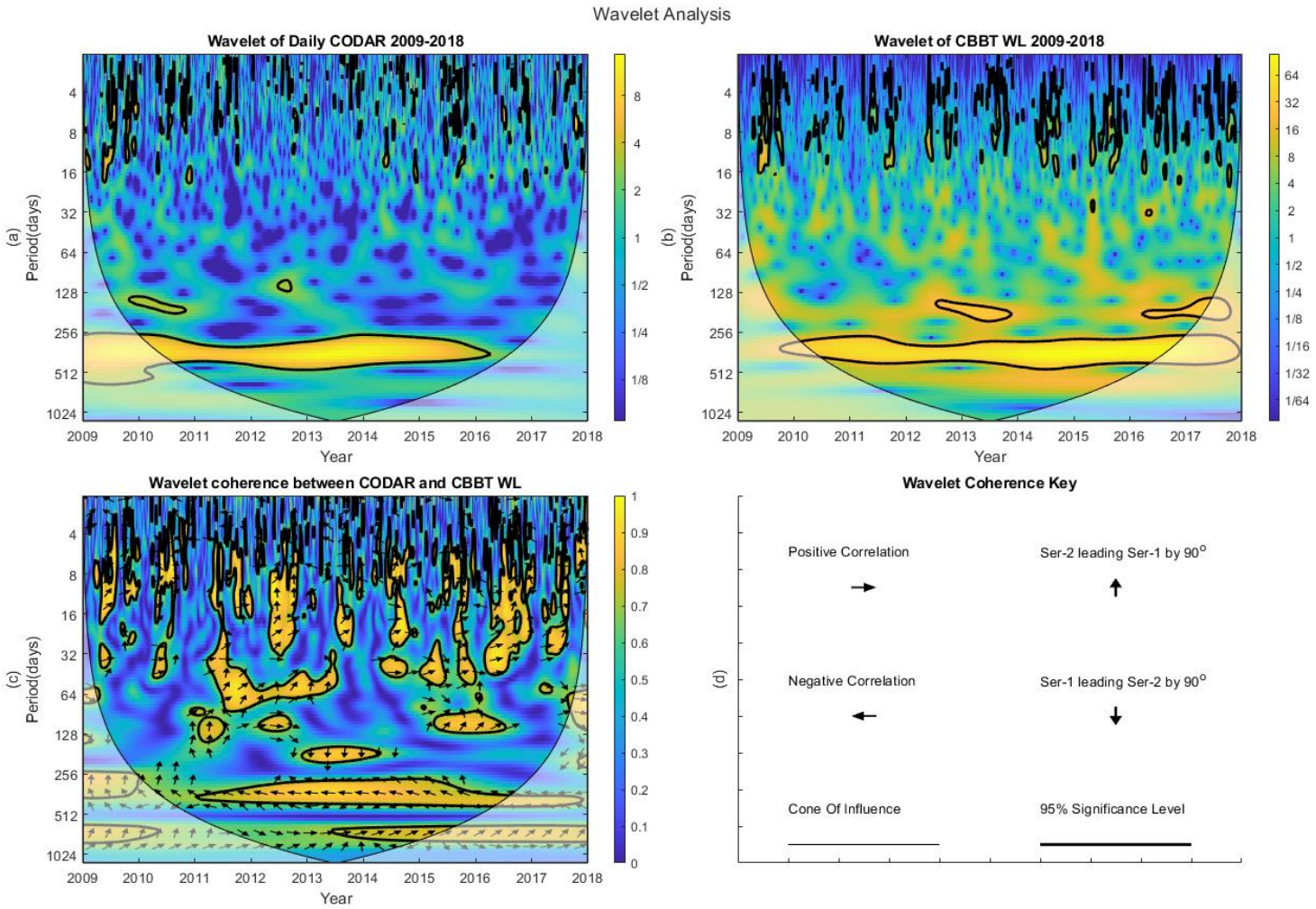

Figure 15: Wavelet analysis of the daily time series of averaged CODAR currents out of the CB (a). Wavelet analysis of the daily time series of water level, as measured at the CBBT (b). Strong power is indicated by yellow and decreases along the colorbar. Cross wavelet transform and coherence (c) indicates shared power and direct correlation between the two time series. Arrows indicate positive, negative, or lagged relationships and thick contours indicate 95% significance, as depicted by the key (d).

Table 3: Consolidation of three analyses' comparing the CODAR surface currents out of the Chesapeake Bay to water level inside the Bay. The EMD correlation coefficient R is a range of values taken from the correlations of the 3 tide gauge stations. Spectral and wavelet analyses' capture cycles less than 2.5 years, while EMD captures oscillations on scales the length of the time series.

	Spectral Coherence		**EMD Cross Correlation**		**Wavelet**
Period	*Coherence²*	*Phase*	*R*	*Significance*	*Coherence*
Daily/Weekly ***T≈ 0-14 days***	0.58 – 0.81	0^o– -137^o	0 – 0.08	> 90%	Nonstationary & variable
Monthly ***T≈ 30-90 days***	0.66	-25^o	-0.06 – 0.08	> 85%	Nonstationary & variable
Semi-Annual ***T≈ 180 days***	0.16	N.S.	-0.31 – -0.39	> 95%	Nonstationary & variable
Annual ***T≈ 360 days***	0.47	N.S.	-0.02 – 0.16	> 70%	Negative
Interannual ***T≈ 2.5 years***	0.03	N.S.	-0.24 – 0.40	< 70%	Positive
Interannual ***T≈ 3.5 years***	N/A	N/A	-0.33 – -0.09	< 70%	N/A
Interannual ***T≈ 4.5 years***	N/A	N/A	-0.07 – 0.26	< 70%	N/A
Decadal ***T≈ 8 years***	N/A	N/A	-0.78 – -0.73	< 70%	N/A

DISCUSSION

WATER LEVELS

Unlike hourly data during a tidal cycle where water level and surface currents are strongly linked and anticorrelated (Fig. 2), daily averaged water levels showed the lowest linear correlation (Table 2) compared to the CODAR surface currents, indicating the height of the water in the lower Bay has little immediate impact on the velocity of the currents moving out of the CB. The relationship, however, is positive, which in part may be due to the progressive nature of the tide at the mouth of the Bay, where maximum tidal height and maximum current occur at the same time. On daily mean basis other forcing may be responsible for most of the CODAR variability.

The spectral analysis of the water level time series (Fig. 7d) and its coherence to the CODAR time series (Fig. 8a) provides additional insight about the relationship and lag that occurs that simple linear correlation does not capture. The sea level time series has peaks in power at frequencies of about one year and one month. Significant power ($C^2 > 0.55$) is shared with the CODAR currents at frequencies of a month and at frequencies between days-weeks. The phase of this coherence is negative, meaning the water levels (tides) are a driving force of currents moving out of the Bay. On weekly scales, the phase is closer to 180º, indicating the relationship is very near anti-correlated and better fits the understanding that lower water levels allow more water to flow out to sea (and vice versa).

The EMD analysis provides an estimated trend and coherence to CODAR at different time scales out to 8 years. While not statistically significant, the final IMF from the water level analysis (Fig. 11b) shows sea level rising, which is qualitatively accurate, particularly in the lower Chesapeake Bay where SLR is estimated to be increasing 3.5-4.4 mm/year (Eggleston et. al, 2013; Boon, 2010; Ezer & Corlett, 2012), and is anti-correlated to the trendline for CODAR. The water level IMF's are most (anti)-correlated to CODAR IMF's on scales of six months (Fig. 12a), which may be indicative of a shared seasonal cycle. This can also be seen in Fig. 6a-b., where the tide gauges and CODAR have opposite monthly averages, for example, maximum water level and slowest currents occurring in September. Correlations between 6-months and 4.5 years (Fig. 12a) between the two datasets are inconsistent, however using monthly averages (Fig. 13a), correlations with periods between 3.5 to 8 years are negative, indicating the two are anti-correlated on longer, decadal time scales.

The wavelet analysis was calculated between only the CODAR and water level datasets as a mean to corroborate findings between the different analysis methods. The wavelet provided results consistent with the spectral analysis, showing shared power between the two on the annual frequency, semi-annual frequency, and variable high frequencies, up to frequencies of about two years (Fig. 17). In comparison to EMD, the wavelet provided more significant results on these scales where the EMD is only

significant up to 6 months. There is some contradiction between the two, for instance, wavelet annual frequency suggests a significant anti-correlation, whereas EMD annual frequency shows insignificant, near-zero, but positive correlation between WL and CODAR. It is likely the EMD cannot capture these scales as well as wavelet. At the 6-month frequency, EMD suggests a negative correlation, but the wavelet shows a non-stationary, inconsistent pattern between the two. More data is needed to produce significant results using EMD or to calculate more consistent results between the three analyses.

WINDS

The greatest linear correlation was found between CODAR and the U-component, or zonal velocity of wind, showing that changes in wind can influence the speed and direction of the surface currents directly (Table 2). In the late fall and winter, when winds are most energetic and primarily from the northwest, the wind pushes water out of the bay and the two are most correlated (Boicourt, 1981).

Spectral analysis of the wind speed and U-wind are very similar to each other and to CODAR, with maximum PSD's at one year and one month (Fig. 7b-c). Unlike the power spectrum of sea level, wind is significantly coherent to CODAR on the annual scale, in addition to the coherency at weekly frequencies (Fig. 8b-c). Cross spectrum phase is negative between the currents and wind, meaning the wind is driving the currents, and with phase being near zero, the relationship is positively correlated.

The EMD analysis produced final (insignificant) trendlines for the wind data that appear largely constant, though are anti-correlated to the trendline for CODAR (Fig. 11c). Both wind speed and U-wind are positively correlated to the currents at high frequencies (hours-weeks) with EMD, which is in agreeance with the spectral analysis (Fig. 12b). Though insignificant on scales later than 6-months, the U-wind component remains positively correlated to currents until scales of 2.5 years, whereas the overall wind speed becomes negatively correlated on scales between weeks-months, likely a result of the V-wind component and seasonal wind shifts (Fig. 12b). Both are positively correlated on semiannual scales, which is indicative of a similar seasonal pattern; this in agreeance given the monthly averages (Fig. 6c-d) which have roughly the same pattern, with the lowest currents and wind occurring in the late summer. On scales out to 8 years, the wind speed and U-wind are interestingly anti-correlated to the CODAR currents (Fig. 13b).

RIVER DISCHARGE

River discharge and the CODAR currents have a positive linear relationship (Table 2), reinforcing the point that increased freshwater from the rivers increases the surface velocity of outflow at the mouth of the Bay. The spectral analysis of river discharge shows peak power at frequencies of one year and one month (Fig. 7e). The power spectrum is significantly coherent to CODAR on the annual and monthly scales, with some coherency at weekly time periods (Fig. 8d). Cross spectrum phase is positive on the annual scale, which would typically indicate the currents precede the river discharge, but this does

not make sense mechanically; perhaps this is a result of seasonal wind or sea level changes occurring before peak river discharge. On the monthly scale, cross spectrum phase is negative and near out of phase, indicating the rivers are driving the currents, but could be anti-correlated at this frequency or more.

The EMD analysis produced a trendline predicting an increase of river discharge to the Chesapeake Bay, which is qualitatively like the previously mentioned climate-related increase in precipitation over the CB watershed (Boomer et. al, 2019), and is positively correlated to the trendline calculated for the CODAR currents (Fig. 11d). However, longer records are needed to evaluate climatic changes. The correlations calculated from the IMF's show little correlation between river discharge and the currents until frequencies between 1-3 months (Fig. 12c) where they are positively correlated. This correlation is likely due the residence time of the water moving from the discharge point in the Bay (mostly upper CB) to the point where flow is measured (lower CB) moving out of the Bay. On time scales between 6 months-4.5 years, the correlation is negative, though correlations after 6-months are considered insignificant. On the other hand, the correlations using the monthly IMF's show a positive correlation on scales after 3.5 years (Fig. 13c), suggesting the two may be negatively correlated on interannual scales, but positively correlated for monthly and decadal time scales.

GULF STREAM

A negative linear relationship exists between the Gulf Stream and the CODAR surface currents (Table 2), but does not necessarily mean a change in the speed of the GS would induce an immediate change in the outflow of surface currents in the CB, as the currents are likely affected by other factors (such as wind and water level).

Spectral analysis of the GS transport shows a peak in PSD on annual and monthly time scales (Fig. 7f), but the GS is coherent with the CODAR PSD on annual and longer time scales as well as on weekly frequencies (Fig. 8e). The cross spectrum phase on the annual scale is positive, though close to out of phase, meaning the two are near anti-correlated at this frequency. There are few peaks that are significant on the weekly scales, though each are close to out of phase (and thus anti-correlated), suggesting that perhaps even on shorter time scales the GS can influence the currents at the mouth of the Bay.

The EMD analysis of the GS produced an unexpected trendline that suggests an increase in GS transport (Fig. 11d), whereas previous studies of the GS have shown a downward trend of transport since 2004 (Ezer et al., 2013; Smeed et al., 2014). What this final IMF is likely showing, more so than a trend, is part of a longer oscillation period of unknown decadal origin. Nevertheless, the trend of increasing CODAR flow out of the bay is consistent with this increase in Gulf Stream transport seen in this EMD analysis, which would cause a local drop in coastal sea level and pull more water out of the Bay (if the time scales aligned) and the two could positively correlated. The correlations calculated between the other

IMF's show little correlation until the 1-3 month range, where the GS and CODAR currents are positively correlated (Fig. 12c). At the 6-month frequency the two series are unexpectedly anti-correlated given the negative correlation to water level; it is possible that at the semiannual time scale other processes are in effect like the seasonal variations of coastal currents or delay response of the CB to changes in the GS upstream. For frequencies after 6-months, the correlation is near zero for interannual periods (1-4.5 years) and using monthly averages (Fig. 13c), shows negative correlation on decadal time scales (8 years), opposite to trend prediction (which again, may not truly be a trend but rather part of a decadal oscillation). The difficulty of assessing the relation between the GS and CODAR currents is that the link is indirect (mostly through changes in water level), and remote in location (the Florida Current observations are farther upstream from the Mid-Atlantic Bight). There is also the possibility (not tested here) that the strength and position of the GS influences coastal currents (Ezer, 2015) which impact currents near the mouth of the CB.

CONCLUSION

The goal of the study was to get a better understanding of the different forcing of the surface currents at the mouth of the Chesapeake Bay as measured by CODAR and study the different time scales involved. This goal was achieved by using several statistical analysis techniques, providing additional information on the usefulness of different analysis methods. The spectral analysis shows that in general high frequency (short time scales) oscillations of CODAR are driven by local tide and wind forcing, while the low frequency oscillations, greater than 3 months, are more likely explained by the indirect forcing of river discharge and the Gulf Stream. Since our data set is only nine years in length, the spectral analysis can only capture signals of about two years, while EMD analysis was applied to attempt to detect oscillations and trends on longer time scales.

The EMD analysis did not provide significant new information regarding the relationship between CODAR and the other time series that was not captured within the linear regression, spectral, and wavelet analyses, as correlations for time scales longer than 6-months were not very statistically significant. Nevertheless, qualitatively, some of the changes seen in the final IMF's of the datasets, representing the trend, are consistent with the dynamics involved to include increasing sea level and river discharge. The final IMF's for Gulf Stream transport and CODAR surface current velocity are likely part of larger decadal oscillations of unknown origin not captured within this nine-year dataset more so than an overall trend. The high frequency oscillations from the EMD analysis agree with spectral analysis showing predominantly positive correlations to U-wind/wind speed and water level, suggesting that these factors are largely driving the surface currents on time scales of days to weeks. On approximately monthly time scales, both river outflow and GS speed have positive correlations, suggesting a delayed response relationship or shared seasonality. At the semi-annual period, the speed of the Gulf Stream and water level are both anti-correlated to the CODAR currents, suggesting that the relationship between the GS and water level is affected by other processes such as seasonal variations or a delayed response between water level and the GS upstream. A look at the monthly correlations suggest that the low frequency (decadal) oscillations are controlled by local water level, river discharge, and the Gulf Stream.

Though insignificant, the long term EMD results from this study show that the CODAR data has the potential to detect and monitor long-term changes in the currents and possibly use correlations to monitor sea level changes in the Chesapeake Bay given significant correlations can be calculated at long time scales to sea level, wind, river discharge, and the Gulf Stream transport. Given a longer dataset, EMD may be able to calculate these significant oscillations and correlations, particularly on scales that spectral and wavelet analysis cannot capture, that could be useful to monitor the Chesapeake Bay or be used in numerical modeling of the Bay for long-term forecasting and trend analysis. Though not studied in this thesis, there is also the potential to study spatial changes in surface flow within the 2-D velocity

maps and how it relates these various forcings as well. Seasonal correlations are not calculated in this study but would also be worth researching at in the future.

In summary, the study demonstrated the complex nature and interconnections between the different factors affecting the currents at the mouth of the Chesapeake Bay, such as water level, winds, rivers, and the Gulf Stream. This analysis may be the first of its kind in the attempt at combining all these different observations in a single study. While some results are expected, such as the general influence of winds and tides on surface currents, the interpretation of the results was not always clear due to variability over different time scales and some disagreement between different analysis methods.

REFERENCES

Ahnert, F. (1960). Estuarine Meanders in the Chesapeake Bay Area. Geographical Review, Vol. 50, No. 3, pp. 390–401. JSTOR, www.jstor.org/stable/212282.

Atkinson, L.P, Garner, T., Blanco, J., Paternostro, C., and Burke, P. (2009). HFR surface currents observing system in lower Chesapeake Bay and Virginia coast, OCEANS 2009, Biloxi, MS, pp. 1-6, doi: https://doi.org/10.23919/OCEANS.2009.5422254

Baringer, M.O. and Larsen J.C. (2001). Sixteen years of Florida Current Transport at 27^o N, Geophysical Research Letters, Volume 28, Issue 16. https://doi.org/10.1029/2001GL013246

Boomer, K., Boynton, W., Muller, A., Muller, D., and Sellner K. (2019). Revisiting Coastal Land-Water Interactions: The Triblet Connection. STAC Publication Number 19-005, Edgewater, MD. pp 37.

Boon, J. D., Brubaker, J. M., & Forrest, D. R. (2010). Chesapeake Bay Land Subsidence and Sea Level Change : an evaluation of past and present trends and future outlook. Special report in applied marine science and ocean engineering; no. 425. Virginia Institute of Marine Science, William & Mary, doi: https://doi.org/10.21220/V58X4P

Chesapeake Bay Program. (2021). Facts and Figures. https://www.chesapeakebay.net/discover/facts

CODAR Ocean Sensors. (2020). About CODAR. http://www.codar.com/about.shtml

Coughlin, K. and Tung, K.K. (2005). Empirical Mode Decomposition of Climate Variability. University of Washington, Department of Applied Mathematics. http://depts.washington.edu/amath/faculty/tung/journals/coughlin-tungHHT05.pdf

Eggleston, J. and Pope, J. (2013). Land subsidence and relative sea-level rise in the southern Chesapeake Bay region: U.S. Geological Survey Circular 1392, p.30, doi: https://dx.doi.org/10.3133/cir1392.

Ezer, T. (2020). Analysis of the changing patterns of seasonal flooding along the U.S. East Coast, Ocean Dynamics, 70(2), 241-255, doi:10.1007/s10236-019-01326-7.

Ezer, T. and Dangendorf, S. (2020). Global sea level reconstruction for 1900–2015 reveals regional variability in ocean dynamics and an unprecedented long weakening in the Gulf Stream flow since the 1990s, Ocean Science.

Ezer, T. and L. P. Atkinson. (2014). Accelerated flooding along the U. S. East Coast: On the impact of sea level rise, tides, storms, the Gulf Stream and the North Atlantic Oscillations. Earth's Future, 2(8), 362-382, doi:10.1002/2014EF000252.

Ezer, T., Atkinson, L.P., Corlett, W.B., and Blanco, J.L. (2013). Gulf Stream's induced sea level rise and variability along the US mid-Atlantic coast, Journal of Geophysical Research: Oceans.

Ezer, T., and Corlett, W. B. (2012), Is sea level rise accelerating in the Chesapeake Bay? A demonstration of a novel new approach for analyzing sea level data, Geophys. Res. Lett., 39, doi: 10.1029/2012GL053435.

Grinsted, A. (2017). Cross Wavelet and Wavelet Coherence Toolbox, doi: https://Grinsted.github.io/wavelet-coherence/

Grinsted, A., Moore, J. C., and Jevrejeva, S. (2004). Application of the cross wavelet transform and wavelet coherence to geophysical time series, Nonlin. Processes Geophys., 11, pp. 561–566, doi: https://doi.org/10.5194/npg-11-561-2004.

Huang N.E., Shen Z., Long S.R., Wu M.C., Shih H.H., Zheng Q., Yen N., Tung C.C., and Liu H.H. (1998). The empirical mode decomposition and the Hilbert spectrum for nonlinear and non-stationary time series analysis. Proc. R. Soc. Lond. A.454, pp. 903–995, doi: https://doi.org/10.1098/rspa.1998.0193

Kenigson, J. S., and Han, W. (2014). Detecting and understanding the accelerated sea level rise along the east coast of the United States during recent decades, J. Geophys. Res. Oceans, 119, 8749–8766, doi:10.1002/2014JC010305.

Meinen, C.S., Baringer, M.O., and Garcia, R.F. (2010). Florida Current transport variability: An analysis of annual and longer-period signals, Deep Sea Research Part I: Oceanographic Research Papers, Volume 57, Issue 7, pp. 835-846, doi: https://doi.org/10.1016/j.dsr.2010.04.001

McDuff, R.E. and Heath, G.R. (2001). University of Washington, Oceanography 540 Pages. http://www2.ocean.washington.edu/oc540/lec01-26/

Prokoph, A., El Bilali, H. (2008). Cross-Wavelet Analysis: a Tool for Detection of Relationships between Paleoclimate Proxy Records. Math Geosci 40, pp. 575–586, doi: https://doi.org/10.1007/s11004-008-9170-8

Smeed, D. A., McCarthy, G. D., Cunningham, S. A., Frajka-Williams, E., Rayner, D., Johns, W. E., Meinen, C. S., Baringer, M. O., Moat, B. I., Duchez, A., and Bryden, H. L. (2014). Observed decline of the Atlantic meridional overturning circulation 2004–2012, Ocean Sci., 10, 29–38, doi: https://doi.org/10.5194/os-10-29-2014.

Thiebaux, H. J. and Zwiers, F. W. (1984). The interpretation and estimation of effective sample size, J. Clim. Appl. Meteorol., 23, 800–811.

Thomson, R.E. and Justice, W.E. (1998). Data Analysis in Physical Oceanography.

Torrence, C., & Compo, G. P. (1998). A Practical Guide to Wavelet Analysis, Bulletin of the American Meteorological Society, 79(1), 61-78.

Updyke, T.G., and Atkinson, L.P. (2015) Extreme and Non-Tidal Events in the Chesapeake Bay High Frequency Radar Surface Currents Record.

Valle-Levinson, A., Wong, K., Bosley, K.T. (2001). "Observations of the wind-induced exchange at the entrance to Chesapeake Bay," Journal of Marine Research, Volume 59, Number 3, pp. 391-416(26), Sears Foundation for Marine Research, doi: https://doi.org/10.1357/002224001762842253

Wang, D. (1979). Subtidal Sea Level Variations in the Chesapeake Bay and Relations to Atmospheric Forcing. J. Phys. Oceanogr., 9, 413–421, https://doi.org/10.1175/1520-0485(1979)009<0413:SSLVIT>2.0.CO;2

Wang, D. (1979). Wind-Driven Circulation in the Chesapeake Bay, Winter, 1975. J. Phys. Oceanogr., 9, 564–572, https://doi.org/10.1175/1520-0485(1979)009<0564:WDCITC>2.0.CO;2.

Ward, S.L., Robins, P.E., Lewis, M.J., Iglesias G., Hashemi, M.R., and Neill, S.P. (2018). Tidal stream resource characterization in progressive versus standing wave systems. Applied Energy, Volume 220, pp 274-285. Doi: https://doi.org/10.1016/j.apenergy.2018.03.059.

Wells, R.C., Bailey, R.K., and Henderson, E.P. (1929). Salinity of the Water of Chesapeake Bay. Shorter contributions to general geology, 105-152, Department of the Interior. https://pubs.usgs.gov/pp/0154c/report.pdf

Wu, Z. and Huang, N.E. (2009). Ensemble empirical mode decomposition: a noise assisted data analysis method, Advances in adaptive data analysis. Advances in Adaptive Data Analysis. Vol. 01, No. 01, pp. 1-41 (2009). Doi: https://doi.org/10.1142/S1793536909000047

Wu Z. and Huang N.E. (2004). A study of the characteristics of white noise using the empirical mode decomposition method. Proc. R. Soc. Lond. A.4601597–1611, doi: https://doi.org/10.1098/rspa.2003.1221.

Xiong, Yi. (2010). Chesapeake Bay Tidal Characteristics. Journal of Water Resource and Protection, 02, 619-628, doi: 10.4236/jwarp.2010.27071

VITA

Shelby Kathryn Henderson

Department of Ocean and Earth Sciences, Old Dominion University
406 Oceanography and Physical Sciences Building, Norfolk, VA 23529

EDUCATION

OLD DOMINION UNIVERSITY, NORFOLK, VIRGINIA
Master of Science, Department of Ocean and Earth Sciences, August 2021
Advisor: Dr. Tal Ezer

UNITED STATES COAST GUARD ACADEMY, NEW LONDON, CONNECTICUT
Bachelor of Science, May 2015
Major: Marine Environmental Science

PROFESSIONAL EXPERIENCE:

2015-2017 **Deck Watch Officer,** *USCGC DOUGLAS MUNRO (WHEC-724)*
2017-2019 **Commanding Officer,** *USCGC SAWFISH (WPB-87357)*